NASA Technical Memorandum 83185

Estimation of Airplane Stability and Control Derivatives From Large Amplitude Longitudinal Maneuvers

James G. Batterson
Langley Research Center
Hampton, Virginia

National Aeronautics
and Space Administration

**Scientific and Technical
Information Branch**

1981

SUMMARY

A technique is presented for the estimation of airplane longitudinal stability and control derivatives over a broad range of angle of attack using data from a single large amplitude longitudinal maneuver. The application of a modified stepwise regression algorithm to both a complete data string and to that same data partitioned into bins as a function of angle of attack is demonstrated. Results from the large-scale maneuver agree well with results from 20 maneuvers in which small perturbations from trim at various angles of attack were induced.

INTRODUCTION

There has been considerable interest recently in the poststall and spin flight regimes of airplanes. The inherently nonlinear nature of the aerodynamic forces and moments of these flight regimes create difficulties for both the design of flight test programs and the application of parameter extraction algorithms. Though interest and attention have been high, no consistently reliable method of parametric model identification which can be applied to the transient data collected from stall/spin/high-α (angle of attack) maneuvers has been developed. It is important to be able to build an airplane mathematical model that encompasses all operating regimes. Hence, one must find a method of extracting information from the short-lived stall/spin/high-α maneuvers in order to confirm a given model or build a new model for predicting airplane behavior.

The identification of airplane stability and control parameters across a broad range of flight conditions can be tedious and costly in manpower, computer time, and in-flight time. Moreover, parameters cannot be identified by traditional methods in all flight regimes. In particular, near stall (both prestall and poststall) regimes and spin entry regimes are often too transient (short lived) to provide enough data for analysis by existing techniques. This paper offers a new application of the stepwise regression technique that promises to be useful in previously nonidentifiable flight regimes.

The usual method of parameter identification from flight test consists of first trimming the test airplane to some given equilibrium flight condition (such as $\alpha = \alpha_o$, $v_o = p_o = q_o = r_o = \phi_o = 0$). Then one or more control surfaces (viz, elevator, rudder, aileron) are activated slightly but sharply from their trim position and back to that position. The resulting motion of the airplane is recorded along with the control movement. The data string for such a maneuver is usually 5 to 15 sec long. At data rates of 20 points/sec, the experimenter will then have 100 to 300 points to analyze.

Unfortunately, it is not possible to trim a given airplane at all angles of attack. Moreover, the passage through certain flight regimes is so fleeting that only a few data points are available. In regions where the airplane can be trimmed and the typical maneuvers can be performed, there is a need to know which of the regions provide the most interesting and perhaps nonlinear behavior and hence require the closest scrutiny.

These problems can be solved, as this paper demonstrates, by judiciously using the data obtained from several large amplitude maneuvers. It is shown that for large

amplitude longitudinal maneuvers initiated from $\alpha_o \approx 2.3°$, one can discern information on the behavior of the airplane in several regions of angle of attack. In this way transient behavior can be analyzed as to tentative model structure and parameter values.

Though the linear model of the airplane is sufficient for small perturbations from equilibrium conditions at low angle of attack, there is little known of the proper aerodynamic model at higher angle of attack. Klein has shown in reference 1 that at high lift coefficient C_L, the linear model is inadequate for a general aviation airplane. In the general case of large excursion in the state variables or coupling between angle of attack and lateral motion, Thomas has postulated a need for a nonlinear aerodynamic model. (See ref. 2.)

The maneuvers treated in this paper involve, by their intent, large excursions in α. Such large excursions then encompass regions of both high and low C_L. Hence part of the identification process required in this work is that of model structure determination.

The determination of model structure consists of two basic requirements:

1. Is a linear model adequate?

2. If the linear model is not adequate, which nonlinear terms must be included to provide an adequate model?

Requirements 1 and 2 are addressed by a modified stepwise regression procedure. The stepwise regression is used to enter variables into a regression equation one at a time. The modified stepwise regression considers only the linear model terms first, after which all candidate nonlinear terms are considered. Upon entry of a nonlinear term, superfluous linear terms may be deleted from the model.

The first section of this report deals with the stepwise regression as it is applied to the airplane identification problem. Next, the results of the data analysis are discussed in detail. And, finally, a concluding section summarizes the data analysis and interprets some of the programmatic aspects of the technique used. The equations of motion are presented in an appendix.

SYMBOLS

b span, m

C_L lift coefficient, $L/\bar{q}S$

C_l rolling-moment coefficient

C_m pitching-moment coefficient, $M_Y/\bar{q}S\bar{c}$

C_m' defined in appendix

C_n yawing-moment coefficient

C_X longitudinal-force coefficient, $F_X/\bar{q}S$

C_Y side-force coefficient, $F_Y/\bar{q}S$

C_Z normal-force coefficient, $F_Z/\bar{q}S$

$\bar{c}$ mean aerodynamic chord, m

$E(\ )$ expectation value

F_P partial statistical F-value, standard errors

F_X, F_Y, F_Z force along X, Y, and Z body axis, respectively, N

g acceleration due to gravity, m/sec^2

I_X, I_Y, I_Z moment of inertia about X, Y, and Z body axis, respectively, $kg\text{-}m^2$

I_{XZ} product of inertia, $kg\text{-}m^2$

J error metric

L lift, N

MS_R mean square due to regression

M_Y pitching moment, N-m

m mass, kg

N number of data points

p body axis roll rate, rad/sec

q body axis pitch rate, rad/sec

$\bar{q}$ dynamic pressure

r body axis yaw rate, rad/sec

$r_{x_j y}$ correlation coefficient between x_j and y

$r_{yx_k \cdot x_j x_m x_p}$ correlation coefficient between x_k and y given that x_j, x_m, and x_p are already in regression

S wing area, m^2

t_i ith time interval

u,v,w velocity along X, Y, and Z body axis, respectively, m/sec

V airplane total velocity, m/sec

X N × P matrix of N measurements of P model variables

x_i ith independent model variable

x_{ij} ijth element of X

y dependent variable

$\vec{y}$ $N \times 1$ vector of N measurements of dependent variable

α angle of attack, rad or deg, as appropriate

$\bar{\alpha}$ mean value of angle of attack for a bin, deg

α_i value of α at ith measurement, rad

β angle of sideslip, rad (δ_e produces nose-up pitching moment)

$\Delta\alpha_i$ $= \alpha_i - \alpha_o$, rad

δ_e elevator deflection, rad (standard sign convention)

$\vec{\varepsilon}$ $N \times 1$ error vector

θ pitch angle, rad

$\vec{\theta}$ $P \times 1$ parameter vector

θ_i ith element of $\vec{\theta}$

ρ air density, kg/m^3

ϕ bank angle, rad

Subscript:

o trim value

Supercripts:

T transposed matrix

• derivative with respect to time

Derivatives:

$$C_{m_q} = \frac{\partial C_m}{\partial q \; \bar{c}/2V} \qquad C_{m_{q\alpha}} = \frac{\partial^2 C_m}{\partial q \; \partial \alpha \; \bar{c}/2V} \qquad C_{m_\alpha} = \frac{\partial C_m}{\partial \alpha}$$

$$C_{m_{\dot{\alpha}}} = \frac{\partial C_m}{\partial \dot{\alpha} \; \bar{c}/2V} \qquad C_{m_{\delta_e}} = \frac{\partial C_m}{\partial \delta_e}$$

$$C_{m_{\delta_e \alpha}} = \frac{\partial^2 C_m}{\partial \delta_e \; \partial \alpha} \qquad C_{m_{\beta^2}} = \frac{1}{2} \frac{\partial^2 C_m}{\partial \beta^2} \qquad C_{m_{\beta^2 \alpha}} = \frac{1}{2} \frac{\partial^3 C_m}{\partial \alpha \; \partial \beta^2}$$

$$C_{m_{\alpha^i}} = \frac{1}{i!} \frac{\partial^i C_m}{\partial \alpha^i} \qquad (i = 2, 3, \ldots, 8)$$

$$C_{Z_q} = \frac{\partial C_Z}{\partial q \, \bar{c}/2V} \qquad C_{Z_{q\alpha}} = \frac{\partial^2 C_Z}{\partial \alpha \, \partial q \, \bar{c}/2V} \qquad C_{Z_\alpha} = \frac{\partial C_Z}{\partial \alpha}$$

$$C_{Z_{\delta_e}} = \frac{\partial C_m}{\partial \delta_e} \qquad C_{Z_{\delta_e \alpha}} = \frac{\partial^2 C_Z}{\partial \alpha \, \partial \delta_e} \qquad C_{Z_{\beta^2}} = \frac{1}{2} \frac{\partial^2 C_Z}{\partial \beta^2}$$

$$C_{Z_{\beta^2 \alpha}} = \frac{1}{2} \frac{\partial^3 C_Z}{\partial \alpha \, \partial \beta^2} \qquad C_{Z_{\alpha^i}} = \frac{1}{i!} \frac{\partial^i C_Z}{\partial \alpha^i} \qquad (i = 2, 3, \ldots, 8)$$

MODEL SELECTION AND PARAMETER ESTIMATION

A stepwise linear regression was applied to the data for both model selection and the estimation of the parameters comprising the model. A general discourse on regression (equation error) techniques is found in reference 3. The stepwise procedure employed for this report is basically that given on pages 178 through 195 in reference 4. In general, a probabilistic parameter estimation method such as maximum likelihood is preferred to a regression method. However, as part of the analysis for this report, the data were partitioned, destroying its continuous dynamic properties over more than a few points. Hence, such probabilistic methods were not applicable. Moreover, if the model be correct and model variable measurement error small, the regression technique gives reasonable results. (See ref. 1.)

System identification is divided by Zadeh (ref. 5) into several major areas. Two areas that this report considers are model selection and parameter identification.

In the standard linear regression technique, a measured quantity, y, is expressed as a function of several independent variables, x_i $(i = 1, \ldots, P)$, and multiplicative coefficients, θ_i $(i = 1, \ldots, P)$, as

$$y = \theta_1 + \theta_2 x_2 + \theta_3 x_3 + \ldots + \theta_p x_p \qquad (1)$$

Equation (1) is derived in the appendix where y corresponds to an aerodynamic force coefficient or moment coefficient; the variables x_i correspond to the model variables α, q, δ_e, and their combinations; the coefficients θ_i represent the aerodynamic stability and control derivatives such as C_{Z_α}, C_{Z_q}, $C_{Z_{\delta_e}}$, C_{m_α}, C_{m_q}, and $C_{m_{\delta_e}}$. If measurements are made on all variables at times $t_1, t_2, \ldots, t_N$, then equation (1) can be written as N independent equations:

$$\left.\begin{aligned} y_1 &= \theta_1 + \theta_2 x_{12} + \theta_3 x_{13} + \ldots + \theta_P x_{1P} \\ y_2 &= \theta_1 + \theta_2 x_{22} + \theta_3 x_{23} + \ldots + \theta_P x_{2P} \\ &\vdots \\ y_N &= \theta_1 + \theta_2 x_{N2} + \theta_3 x_{N3} + \ldots + \theta_P x_{NP} \end{aligned}\right\} \tag{2}$$

which can be summarized in the matrix equation:

$$\vec{y} = X\vec{\theta} \tag{3}$$

where $\vec{y}$ is an $N \times 1$ vector of the N measurements of the dependent variable, X is an $N \times P$ matrix whose jth column contains the N measurements of the jth model variable, and $\vec{\theta}$ is a $P \times 1$ parameter vector (unknown).

Because of error associated with the measurement of y_i, the linear combination of model variables may not faithfully represent the system. Hence, one must associate an $N \times 1$ error vector $\vec{\epsilon}$ with equation (3) to give

$$\vec{y} = X\vec{\theta} + \vec{\epsilon} \tag{4}$$

where $\vec{\epsilon}$ is referred to as the "equation error" and often lends that name to the linear regression method. If $\vec{\epsilon}$ is stationary white, zero mean, and the elements of X are measured without error, then the regression technique gives

unbiased parameter estimates $\hat{\theta} = [X^T X]^{-1} X^T \vec{y}$ when the cost function

$J = \vec{\epsilon}^T \vec{\epsilon} = (\vec{y} - X\vec{\theta})^T (\vec{y} - X\vec{\theta})$ is minimized with respect to $\vec{\theta}$. That is,

$E(\vec{\epsilon}^T X) = \vec{0}$ is desired. To achieve this, one must have the correct model postulated in equation (1). Usually, for small longitudinal perturbations, a simple linear model, incorporating only the model variables α, q, and δ_e, will suffice. However, for larger perturbations from equilibrium flight and/or for high C_L, it has been shown that certain nonlinear combinations of the model variables might be required. (See ref. 1.)

Candidate combinations of the model variables are listed in table 1. The candidate model variables consist of the linear terms α, q, and δ_e and certain nonlinear terms. The first three nonlinear terms are α^2, αq, and $\alpha\delta_e$ which yield parameters corresponding to the slope of the linear parameters with respect to α. Next, two terms which account for symmetrical coupling of the longitudinal motion with sideslip (viz, β^2 and $\beta^2\alpha$) are considered. Finally, since the longitudinal motion is generally most dependent on α, the higher order terms α^3, ..., α^8 are included. If all the candidate variables listed are included, another problem is

created: the $[X^TX]$ matrix is singular and $\hat{\theta}$ does not exist. Therefore, one must include enough variables to postulate the correct model $E(\vec{\varepsilon}^T X) \approx \vec{0}$ but not so many variables that $[X^TX]$ is made singular.

It is desirable then, to add variables to the model, one at a time, until the model is correct. A stepwise regression does exactly that. In a stepwise regression, the equation error is decreased in "steps" by adding the independent model variables to the model one at a time. One begins the procedure by postulating a one parameter model

$$\vec{y} = \hat{\theta}_1 + \vec{\varepsilon}$$

where $\hat{\theta}_1$ is simply the mean of the data. A tableau of candidate independent model variables, $x_2, x_3, \ldots, x_p$ is available. The tableau for the airplane longitudinal equations of motions is given by table 1.

Next the correlation coefficients

$$r_{x_j y} = \frac{\sum_{i=1}^{N} x_{ij} y_i}{\sqrt{\sum_{i=1}^{N} x_{ij}^2 \sum_{i=1}^{N} y_i^2}}$$

are calculated for each x_j $(j = 1, \ldots, P)$. Then the x_j corresponding to the greatest $r_{x_j y}$ is selected to enter the regression. Now the model is

$$\vec{y} = \hat{\theta}_1 + \hat{\theta}_j \vec{x}_j + \vec{\varepsilon}$$

Next, the correlation coefficient for each remaining x_i $(i = 2, \ldots, j-1, j+1, \ldots, P)$ is calculated on x_j and $\hat{y}$ where $\hat{y} = \hat{\theta}_1 + \hat{\theta}_j \vec{x}_j$. The correlation coefficient is

$$r_{y x_k \cdot x_j} = \frac{\sum_{i=1}^{N} \left(x_{ik} - x_{ij}\hat{\theta}_j - \hat{\theta}_1\right)\left(y_i - \hat{y}_i\right)}{\sqrt{\sum_{i=1}^{N} \left(x_{ik} - x_{ij}\hat{\theta}_j - \hat{\theta}_1\right)^2 \sum_{i=1}^{N} \left(y_i - \hat{y}_i\right)^2}}$$

$r_{yx_k \cdot x_j}$ is read the partial correlation of y on x_k given that x_j is in the regression.

The x_k giving the largest value of $r_{x_k y \cdot x_j}$ is selected and entered into the model. The model is now

$$y = \hat{\theta}_1 + \hat{\theta}_j x_j + \hat{\theta}_k x_k$$

Again a partial correlation coefficient, $r_{x_\ell y \cdot x_j x_k}$ is calculated and the x_ℓ giving the largest $r_{x_\ell y \cdot x_j x_k}$ enters the model. This process continues until the remaining candidate variables offer no statistical improvement in the model at a level of significance selected by the user.

At each step of the regression, one has several pieces of information available. First, the most obvious is the model structure. Second, there is a least-squares estimate of the parameters for each model selected. Third, the F-value of significance can be calculated by

$$F = \frac{MS_R}{S}$$

Fourth, a partial F value F_p given by

$$F_p = \frac{N - m}{m - 1} \frac{r_{yx_k \cdot x_j}}{1 - r_{yx_k \cdot x_j}}$$

is calculated giving the relative statistical significance of each variable in each model, given that the other variables are present.

The stepwise regression used for this analysis differs slightly from that in reference 4. Hence, it is required that the linear model (that model containing only α, q, and δ_e) be fit first and the nonlinear terms considered next. This constraint allows the user to view the linear model performance before searching for a more complex model.

The best model is chosen as the one corresponding to the largest total F-value. If that peak is not clear, then the set of F_p's is searched on several of the better candidate models to choose the most consistent and parsimonious model.

Simulated data created from a nonlinear model at high angle of attack have borne out these methods. With no noise on either the dependent or independent variables, the correct model was selected and correct parameter values identified. With noise

on all variables (worst case), the procedure selected the correct model structure in the rolling- and yawing-moment equations. In the side-force equation, two of the nonlinear terms were not selected in the presence of noise; however, no term that did not appear in the true model was selected either. Hence the technique selected, at worst, a parsimonious model and, at best, the true nonlinear model.

DATA ANALYSIS

The data were obtained from a low wing general aviation airplane with a modified wing leading edge. Because of the leading-edge modification, the test airplane could be trimmed at angles of attack that were well above the stall angle of the unmodified wing. Taking advantage of this large range of trim angle of attack, two major data sets were created.

The first data set consists of the results of 21 transient small amplitude longitudinal maneuvers initiated from steady-state flight conditions. The trim values for α in these 21 maneuvers varies from 2.3° to 20.2°. These small amplitude maneuvers were analyzed with respect for the normal-force and pitching-moment coefficients. The parameters, C_{Z_α}, C_{Z_q}, $C_{Z_{\delta_e}}$, C_{m_α}, C_{m_q}, and $C_{m_{\delta_e}}$, extracted from the 21 small amplitude maneuvers are plotted in figure 1.

The second data set consists of several maneuvers made from steady-state flight trimmed at angles of attack of about 2°. From this trim angle, a large elevator pulse was initiated, resulting in a large excursion from the trim α. A comparison of such a large control input and its resultant α deviation with a typical small control input (from the 21 small amplitude runs) and its α deviation is depicted in figure 2.

The second set of data was then analyzed in two ways. In the first analysis, the entire data length from a particular maneuver was analyzed by using the stepwise regression. This technique is the same as the one that was applied to the 21 small amplitude maneuvers. The results of this analysis for two particular large maneuvers (run 18 and run 19) are given in figures 3 and 4. It is seen in the figures that trend lines (dashed lines) have been extrapolated from the trim value of that parameter to higher α values. The trend line reflects first derivative values of the parameter (such as $C_{Z_{q\alpha}}$ and $C_{Z_{\alpha^2}}$) that were selected by the stepwise regression. A comparison of these trends with the small amplitude maneuver parameter estimates is seen in figures 5 and 6. The trend lines linearly interpolate the small amplitude data very well. The trend information is not chosen for all parameters in all maneuvers. In such cases, the trend line is represented by a horizontal trajectory signifying a zero slope for that parameter with α.

To improve upon the trend information or rather to achieve a better resolution of the fine structure of the parameter as a function of α trajectories, a second method of analysis was applied to the large amplitude data.

In this second method, the data from each maneuver were divided into bins as a function of α. That is, all measured data corresponding to $0 \leq \alpha < 4°$ were put into the first bin. Data corresponding to $4° \leq \alpha < 8°$ were put into the second bin and so forth until six bins each of 4° width were filled. Then five new bins for $2° \leq \alpha < 6°$, $6° \leq \alpha < 10°$, and so forth, were created and filled with the corresponding measured data. The number of data points and the mean α value of those

points are given for each bin for runs 18 and 19 in table 2. Each bin was analyzed by using the stepwise regression and the results are given in figures 7 and 8. The 4° bin width as chosen as a means of including enough data in each bin but also to restrict each bin to as small a range of α as possible. The smallest range of α prevents data from several regions of aerodynamic behavior from diluting one another. With greater data rates or longer maneuvers it might be possible to make even more narrow bins.

The results of the bin analysis are overlaid with the small amplitude analysis and the entire large amplitude analysis in figures 9 and 10. The solid circles represent the parameter value extracted for a given bin and is plotted at the mean α for the points in that bin. For certain bins, no linear parameter was extracted; hence not all bins have a representative parameter value. However, certain bins yielded trend information, as in the analysis of the entire data length. The trend lines, where available, are plotted at the mean value of α for the points in that bin. One sees that though the entire run analysis can give a general trend in the parameter behavior at higher α, the partitioning of the data into bins provides a fine structure about that trend. Hence more information can be extracted from the same data by dividing it into bins than by simply analyzing the entire data length.

The ordinate value at which a slope line is plotted in this report is determined by extrapolating the ordinate values of previous bins to achieve a reasonable placement. The temptation to treat the ordinate value as equal to zero in cases where only a slope is identified must be suppressed since zero is not the "best" value for the ordinate but rather represents the value most compatible with the best overall model. Because of correlation among the variables in the adequate model, the ordinate value need not be included as a parameter in the best model in certain cases.

An example will better explain the previous paragraph. Consider the binned results for C_{Z_q} of run 19 as shown in figure 10(a). If one considers the equation

$$C_{Z_q} = 0 + C_{Z_{q\alpha}} (\bar{\alpha} - \alpha_o)$$

and, for example, the 12° to 16° bin ($\bar{\alpha} = 14.4°$) of run 19 would give

$$C_{Z_q} = 0 - 1.82(14.4° - 2.3°) = -22.0$$

when such a formula is used, one develops the plot for C_{Z_q} against α shown in figure 11.

Certainly it is better to use the additional information provided by the surrounding bins (as in figs. 9 and 10). However, it is better still to develop an analytical expression to incorporate the ordinates and slope information from surrounding bins into an optimal polynomial fit through all points, obeying the given slope information. The development of such an expression is currently being studied.

DISCUSSION

For the normal-force equation, it is seen in figures 9(a) and 10(a) that C_{Z_α} can be extrapolated from -4.3 at $\alpha \approx 2.3°$ to -1.3° at $\alpha \approx 20°$ by simply using $\partial^2 C_Z / \partial \alpha^2 = 2C_{Z_{\alpha^2}}$ from the large maneuver entire data length. This general trend corresponds to the C_{Z_α} values extracted from the small amplitude transient maneuvers. However, the behavior between these end points is only approximated by such an analysis. The finer behavior is washed out by the averaging of all the data. When one bins the data, it is seen that the trend from trim to about $\alpha = 7°$ is a slow increase, then a rapid increase in C_{Z_α} between $\alpha = 7°$ and 12°, and again a slower increase from $\alpha = 12°$ to 20°. A similar behavior is seen for C_{Z_q}. Moreover, for both runs 18 and 19, it is seen that slope information $C_{Z_{q\alpha}}$ is extracted from certain bins. The slopes are plotted about the mean α for their respective bins. In run 18, one sees that the slope crosses the overall trend line between $\alpha = 7°$ and 11° reinforcing the information from C_{Z_α} that the system behavior is changing most rapidly in this region. Run 19 gives the general decrease in slope $C_{Z_{q\alpha}}$ after its maximum decrease at $\alpha \approx 9.5°$. For $C_{Z_{\delta_e}}$, the entire run analysis gives no nonzero $C_{Z_{\delta_e \alpha}}$ value. This is represented by the zero slope line in figure 10(a). Though the bins of run 19 provide no additional information, run 18 bins provide a slope $C_{Z_{\delta_e \alpha}}$ at 8.7° and shows that $C_{Z_{\delta_e}}$ is about constant at -0.8 from α_o to about $\alpha = 8°$, and then $C_{Z_{\delta_e}}$ stays constant at about -1 from $\alpha = 9°$ to 20°. The standard error at high α makes an exact measure of $C_{Z_{\delta_e}}$ impossible.

For the pitching-moment coefficient equation, one should refer to figures 9(b) and 10(b). The analysis of the entire data length of run 18 failed to give any nonzero trend information for any of the pitching-moment derivatives. This is noted by the horizontal line representing a zero slope trend. The analysis of the entire data length for run 19 gives trend lines for C'_{m_α} and C'_{m_q}. By binning the data, one sees the interesting fine structure in run 18 for C'_{m_α}. The derivative C'_{m_α} is seen to be reasonably constant from α_o to about 8°. Between $\alpha = 8°$ and 12°, C'_{m_α} drops rapidly, steadies from $\alpha = 12°$ to 15.6° and then rapidly decreases as shown by the existence of $C'_{m_{\alpha 2}}$ for two bins between $\alpha = 16°$ and 20°. Though not as visible, the run 18 behavior is not contradicted by run 19 binned analysis.

The variation of C'_{m_q} about the overall trend line for run 19 shows a rapid increase in C'_{m_q} between $\alpha = 4°$ and 10° in that the binned trajectory cross the trend line in that region. Run 18 adds no new information but also does not contradict run 19. The derivative $C'_{m_{\delta_e}}$ is shown, in the binned analysis of run 19,

to have a constant value of about -1.95 from α_o to $\alpha = 7°$ after which it increases between $\alpha = 7°$ and $10°$ for a new constant value of about -1.6. This behavior, especially in regions of change, is consistent with the behavior of the other derivatives in both the binned data and the 21 small amplitude maneuvers.

One final aspect of the application of the stepwise regression for both large and small amplitude maneuvers performed over a large range of trim angles of attack is shown in figure 11. One can take the average excursion in α to be given by $\frac{1}{N}\sum_{i=1}^{N}(\Delta\alpha_i)^2$ where $\Delta\alpha_i$ is $\alpha_i - \alpha_o$ for the ith value of α in a data string for a given run. The number of terms selected for the optimal model is shown as a function of $\frac{1}{N}\sum_{i=1}^{N}(\Delta\alpha_i)^2$ and α_o for the 21 small amplitude maneuvers and the large amplitude maneuvers.

In the semilog plot in figure 12, points where linear models suffice are represented by circles. Maneuvers which required nonlinear models are denoted by squares. The number in the circle or square is the number of terms present in the adequate model. A line separates the plane into two sections. Below the line one finds that a linear model is generally adequate. Above the line, generally a nonlinear model is required. From the plot one sees that justification of a linear model depends both on the excursion from α_o and the behavior of the system in the neighborhood of α_o. Hence even at large α_o, a linear model suffices for an airplane with a reasonably linear lift curve at that α. Also, at low α_o, a nonlinear model is required if the excursion from α_o is large.

CONCLUDING REMARKS

It has been shown that information regarding the behavior of an airplane at high angles of attack exists in data that results from large amplitude longitudinal maneuvers from a low trim angle of attack. A technique has been demonstrated which allows for the determination of overall trend lines indicating the mean behavior of the longitudinal linear stability and control derivatives over a large range of angle of attack. Though this trend line can be useful for gross estimates of airplane behavior at high angle of attack α, a technique of partitioning the data string was shown to give some fine structure and detail about the trend lines. These detailed estimates from partitioning were shown to be reliable in that they agree with estimates using small perturbation from trim condition in certain regions.

The partitioning is especially useful to detect regions of rapid change in parameter values. The regions are usually indicated by the significant contribution of one or more nonlinear terms into the model. These transient regions are areas that should be more closely investigated by further flight tests. They could be interesting areas of nonlinear behavior involving multiple states or hysteresis. Future research should include means of extracting still more information from these "transient data" regions.

The modified stepwise regression, as presented, has been shown to be reliable in choosing an adequate model. Because it does not test all possible models, one is not assured that he has the absolute best model. However, work with simulated nonlinear

models has shown that the model chosen, even under noisy flight conditions is adequate. Future work should include development of an information criterion for a best model.

Finally, it was shown that in some regions the linear model is the best model, but that over a broader range of flight conditions, a nonlinear model is required. Moreover in certain regions of trim angle of attack α_0 even for small perturbations from trimmed flight, a linear model is inadequate for stability and control analysis.

The techniques presented in this paper show promise for the task of model structure determination and analysis of flight data from transient flight regimes. The future development of information criteria and experience developing a better set of candidate model variables will enable the user to better analyze data from transient maneuvers such as are found in prestall and poststall regimes.

Langley Research Center
National Aeronautics and Space Administration
Hampton, VA 23665
August 17, 1981

APPENDIX

EQUATIONS OF MOTION

The following equations of motion are given in this apperdix.

$$\dot{u} = -qu + rv - g \sin\theta + \frac{\rho V^2 S}{2m} C_X$$

$$\dot{v} = -ru + pw + g \cos\theta \sin\phi + \frac{\rho V^2 S}{2m} C_Y$$

$$\dot{w} = -pv + qu + g \cos\theta \cos\phi + \frac{\rho V^2 S}{2m} C_Z$$

$$\dot{p} = qr\left(\frac{I_Y - I_Z}{I_X}\right) + \frac{I_{XZ}}{I_X}(pq + \dot{r}) + \frac{\rho V^2 Sb}{2I_X} C_l$$

$$\dot{q} = pr\left(\frac{I_Z - I_X}{I_Y}\right) + \frac{I_{XZ}}{I_Y}(r^2 - p^2) + \frac{\rho V^2 S\bar{c}}{2I_Y} C'_m$$

$$\dot{r} = pq\left(\frac{I_X - I_Y}{I_Z}\right) + \frac{I_{XZ}}{I_Z}(\dot{p} - qr) + \frac{\rho V^2 Sb}{2I_Z} C_n$$

$$\dot{\theta} = q \cos\phi - r \sin\phi$$

$$\dot{\phi} = p + (q \sin\phi + r \cos\phi) \tan\theta$$

$$V = \sqrt{u^2 + v^2 + w^2}$$

$$\alpha = \tan^{-1}\frac{w}{u} \qquad \dot{\alpha} \approx \frac{\dot{w}}{u}$$

$$\beta = \sin^{-1}\frac{v}{V} \qquad \dot{\beta} \approx \frac{\dot{v}}{V}$$

where

$$C_Z = C_{Z,o} + C_{Z_\alpha}(\alpha - \alpha_o) + C_{Z_q}\frac{q\bar{c}}{2V} + C_{Z_{\delta_e}}(\delta_e - \delta_{e,o}) + C_{Z_{q\alpha}}(\alpha - \alpha_o)\frac{q\bar{c}}{2V}$$
$$+ C_{Z_{\alpha^2}}(\alpha - \alpha_o)^2 + C_{Z_{\delta_e\alpha}}(\alpha - \alpha_o)(\delta_e - \delta_{e,o}) + C_{Z_{\beta^2}}(\beta - \beta_o)^2$$
$$+ C_{Z_{\beta^2\alpha}}(\beta - \beta_o)^2(\alpha - \alpha_o) + C_{Z_{\alpha^3}}(\alpha - \alpha_o)^3 + C_{Z_{\alpha^4}}(\alpha - \alpha_o)^4$$
$$+ C_{Z_{\alpha^5}}(\alpha - \alpha_o)^5 + C_{Z_{\alpha^6}}(\alpha - \alpha_o)^6 + C_{Z_{\alpha^7}}(\alpha - \alpha_o)^7 + C_{Z_{\alpha^8}}(\alpha - \alpha_o)^8$$

$$C'_m = C'_{m,o} + C'_{m_\alpha}(\alpha - \alpha_o) + C'_{m_q}\frac{q\bar{c}}{2V} + C'_{m_{\delta_e}}(\delta_e - \delta_{e,o}) + C'_{m_{q\alpha}}(\alpha - \alpha_o)\frac{q\bar{c}}{2V}$$
$$+ C'_{m_{\alpha^2}}(\alpha - \alpha_o)^2 + C'_{m_{\delta_e\alpha}}(\delta_e - \delta_{e,o})(\alpha - \alpha_o) + C'_{m_{\beta^2\alpha}}(\beta - \beta_o)^2(\alpha - \alpha_o)$$
$$+ C'_{m_{\beta^2}}(\beta - \beta_c)^2 + C'_{m_{\alpha^3}}(\alpha - \alpha_o)^3 + C'_{m_{\alpha^4}}(\alpha - \alpha_o)^4 + C'_{m_{\alpha^5}}(\alpha - \alpha_o)^5$$
$$+ C'_{m_{\alpha^6}}(\alpha - \alpha_o)^6 + C'_{m_{\alpha^7}}(\alpha - \alpha_o)^7 + C'_{m_{\alpha^8}}(\alpha - \alpha_o)^8$$

where

$$C'_{m,o} = C_{m,o} + C_{m_\alpha^\bullet}\left(\frac{\rho S\bar{c}}{4m}C_{Z,o} + \frac{q\bar{c}}{2V^2}\cos\theta_o\right)$$

$$C'_{m_\alpha} = C_{m_\alpha} + \frac{\rho S\bar{c}}{4m}C_{m_\alpha^\bullet}C_{Z_\alpha}$$

$$C'_{m_q} = C_{m_q} + C_{m_\alpha^\bullet}\left(1 + \frac{\rho S\bar{c}}{4m}C_{Z_q}\right)$$

$$C'_{m_{\delta_e}} = C_{m_{\delta_e}} + \frac{\rho S\bar{c}}{4m}C_{m_\alpha^\bullet}C_{Z_{\delta_e}}$$

$$C'_{m_{q\alpha}} = C_{m_{q\alpha}} + C_{m_\alpha^\bullet}\frac{\rho S\bar{c}}{4m}C_{Z_{q\alpha}}$$

APPENDIX

$$C'_{m_{\alpha^2}} = C_{m_{\alpha^2}} + C_{m_{\dot{\alpha}}} \frac{\rho S \bar{c}}{4m} C_{Z_{\alpha^2}}$$

$$C'_{m_{\delta_e \alpha}} = C_{m_{\delta_e \alpha}} + C_{m_{\dot{\alpha}}} \frac{\rho S \bar{c}}{4m} C_{Z_{\delta_e \alpha}}$$

$$C'_{m_{\beta^2 \alpha}} = C_{m_{\beta^2 \alpha}} + C_{m_{\dot{\alpha}}} \frac{\rho S \bar{c}}{4m} C_{Z_{\beta^2 \alpha}}$$

$$C'_{m_{\beta^2}} = C_{m_{\beta^2}} + C_{m_{\dot{\alpha}}} \frac{\rho S \bar{c}}{4m} C_{Z_{\beta^2}}$$

$$C'_{m_{\alpha i}} = C_{m_{\alpha i}} + C_{m_{\dot{\alpha}}} \frac{\rho S \bar{c}}{4m} C_{Z_{\alpha i}}$$

Assuming steady-state ($v_o = p_o = q_o = r_o = \phi_o = 0$) initial flight conditions the longitudinal equations become

$$\dot{u} = -qw - g \sin \theta + \frac{\rho V^2 S}{2m} C_X$$

$$\dot{w} = qu + g \cos \theta + \frac{\rho V^2 S}{2m} C_Z$$

$$\dot{q} = \frac{\rho V^2 S \bar{c}}{2I_Y} C_m$$

$$\dot{\theta} = q$$

and the longitudinal output can be written as

$$a_X = \frac{1}{g}(\dot{u} + qw + g \sin \theta)$$

$$a_Z = \frac{1}{g}(\dot{w} - qu - g \cos \theta)$$

and for the equation error form, the aerodynamic coefficients can be written as

$$\frac{2gm}{\rho V^2 S} a_X = C_X$$

$$\frac{2gm}{\rho V^2 S} a_Z = C_Z$$

$$\frac{2I_Y}{\rho V^2 S\bar{c}} \dot{q} = C_m'$$

REFERENCES

1. Klein, Vladislav: Determination of Stability and Control Parameters of a Light Airplane From Flight Data Using Two Estimation Methods. NASA TP-1306, 1979.

2. Thomas, H. H. B. M.: A Brief Introduction to Aircraft Dynamics. Aircraft Stability and Control - Volume 1, VKI-LS-80, Von Karman Inst. Fluid Dyn., May 1975.

3. Mendel, Jerry M.: Discrete Techniques of Parameter Estimation. Marcel Dekker, Inc., 1973.

4. Draper, N. R.; and Smith, H.: Applied Regression Analysis. John Wiley & Sons, Inc., c.1966.

5. Zadeh, L. A.: From Circuit Theory to System Theory. Proc. IRE, vol. 50, no. 5, May 1962, pp. 856-865.

TABLE 1.- CANDIDATE MODEL VARIABLES

α	α^2	β^2	α^3
q	αq	$\beta^2\alpha$	α^4
δ_e	$\alpha\delta_e$		α^5
			α^6
			α^7
			α^8

TABLE 2.- $\bar{\alpha}$ AND NUMBER OF DATA POINTS PER BIN

α bin	Run 18		Run 19	
	$\bar{\alpha}$	N	$\bar{\alpha}$	N
0° to 4°	1.8	147	1.53	113
2° to 6°	2.8	136	3.1	116
4° to 8°	6.3	40	6.6	83
6° to 10°	8.7	72	8.1	128
8° to 12°	9.9	90	9.5	114
10° to 14°	11.5	56	11.9	56
12° to 16°	14.6	37	14.4	32
14° to 18°	16.3	43	16.7	34
16° to 20°	18.0	35	18.6	46
18° to 22°	20.6	21	20.1	38
20° to 24°	23.6	16	23.0	11

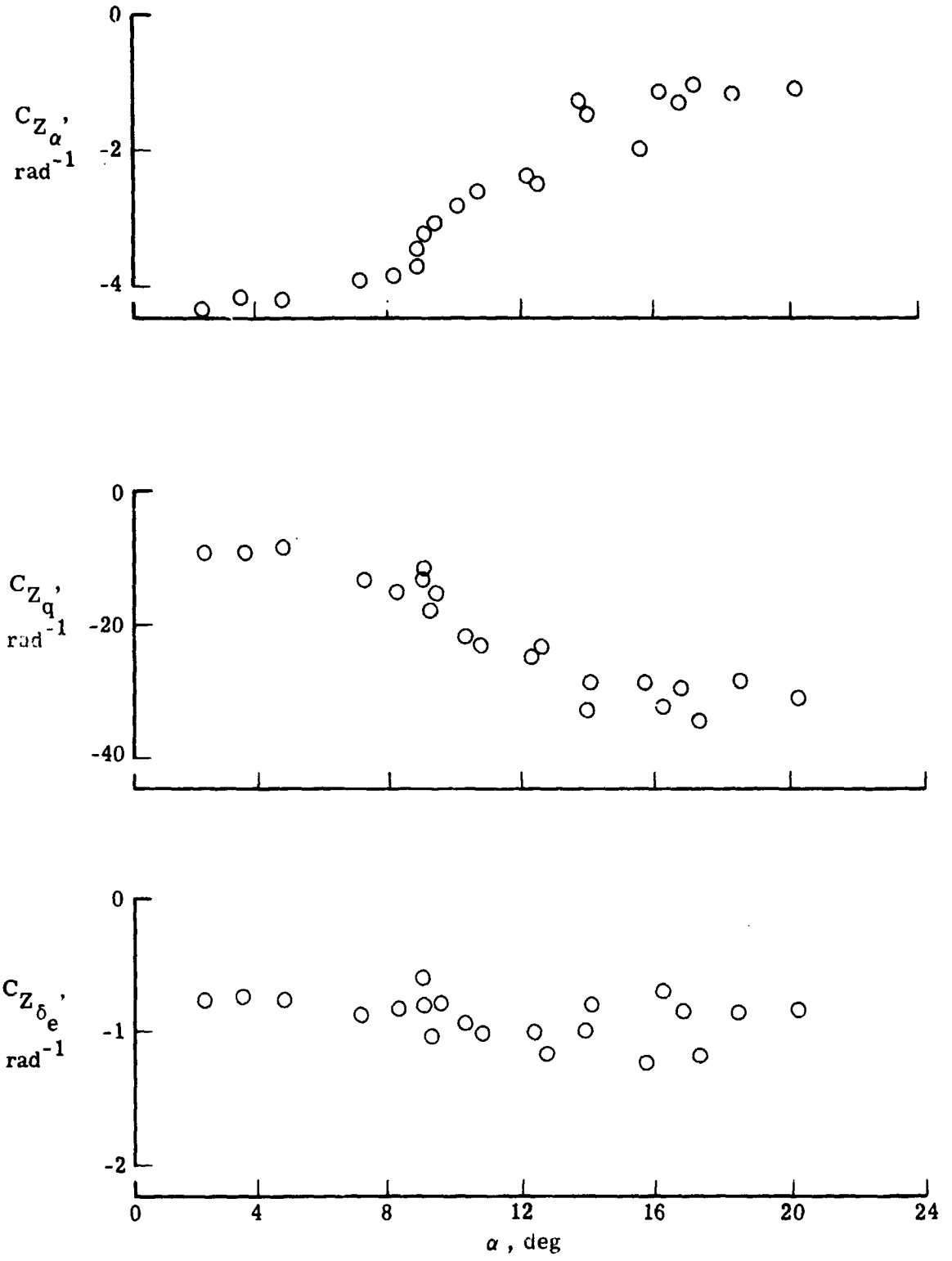

(a) Z-force coefficients.

Figure 1.- Aerodynamic coefficients from small amplitude maneuvers.

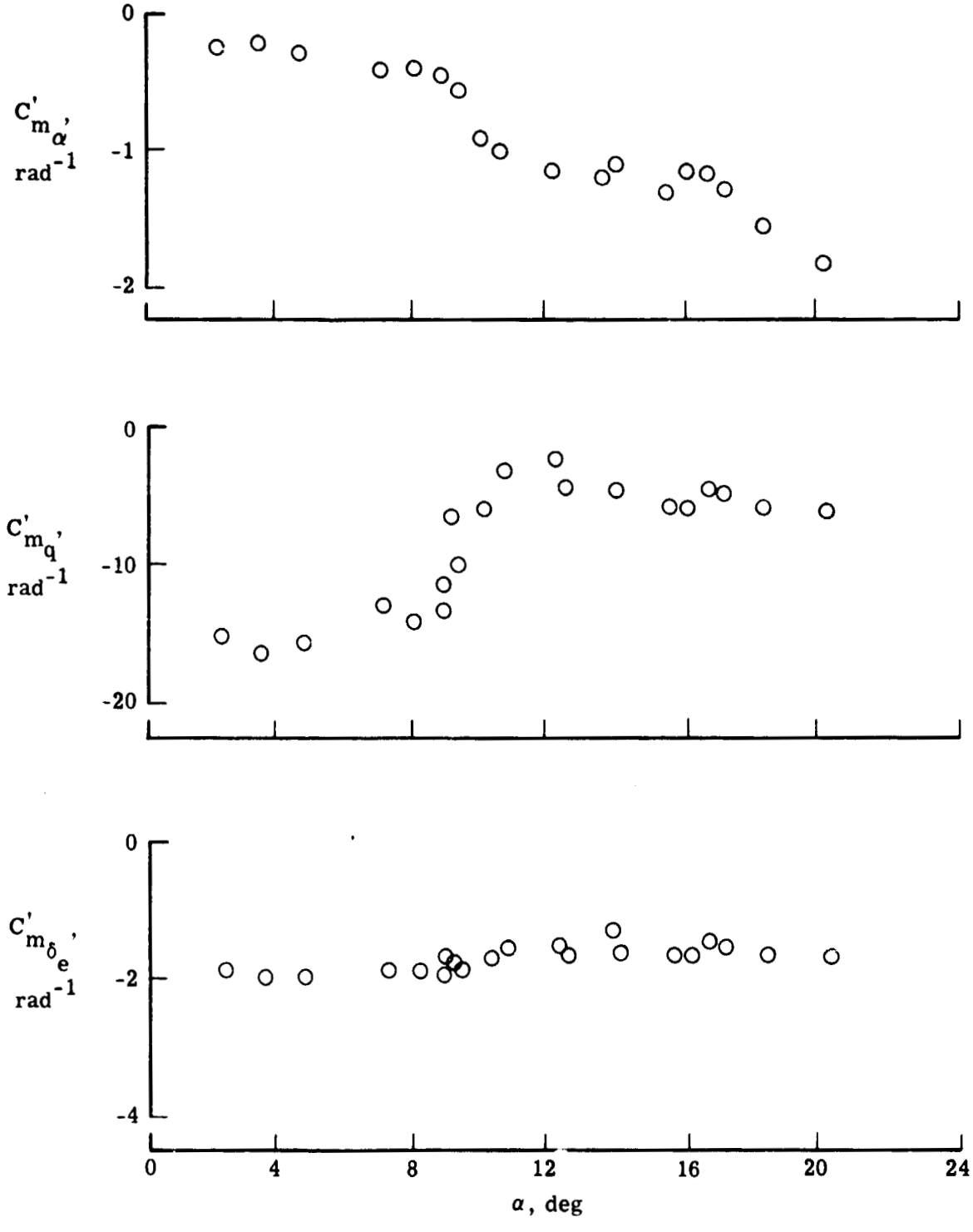

(b) Pitching-moment coefficients.

Figure 1.- Concluded.

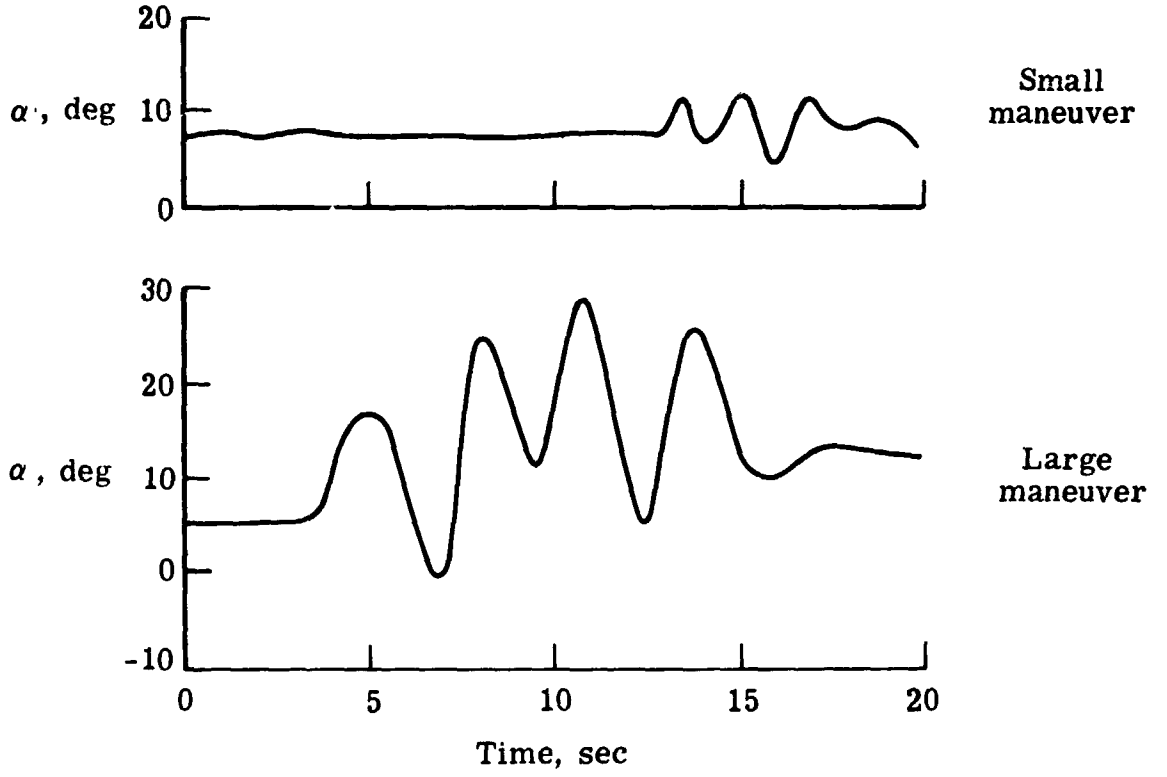

Figure 2.- Comparison of α excursions for typical small and large maneuvers.

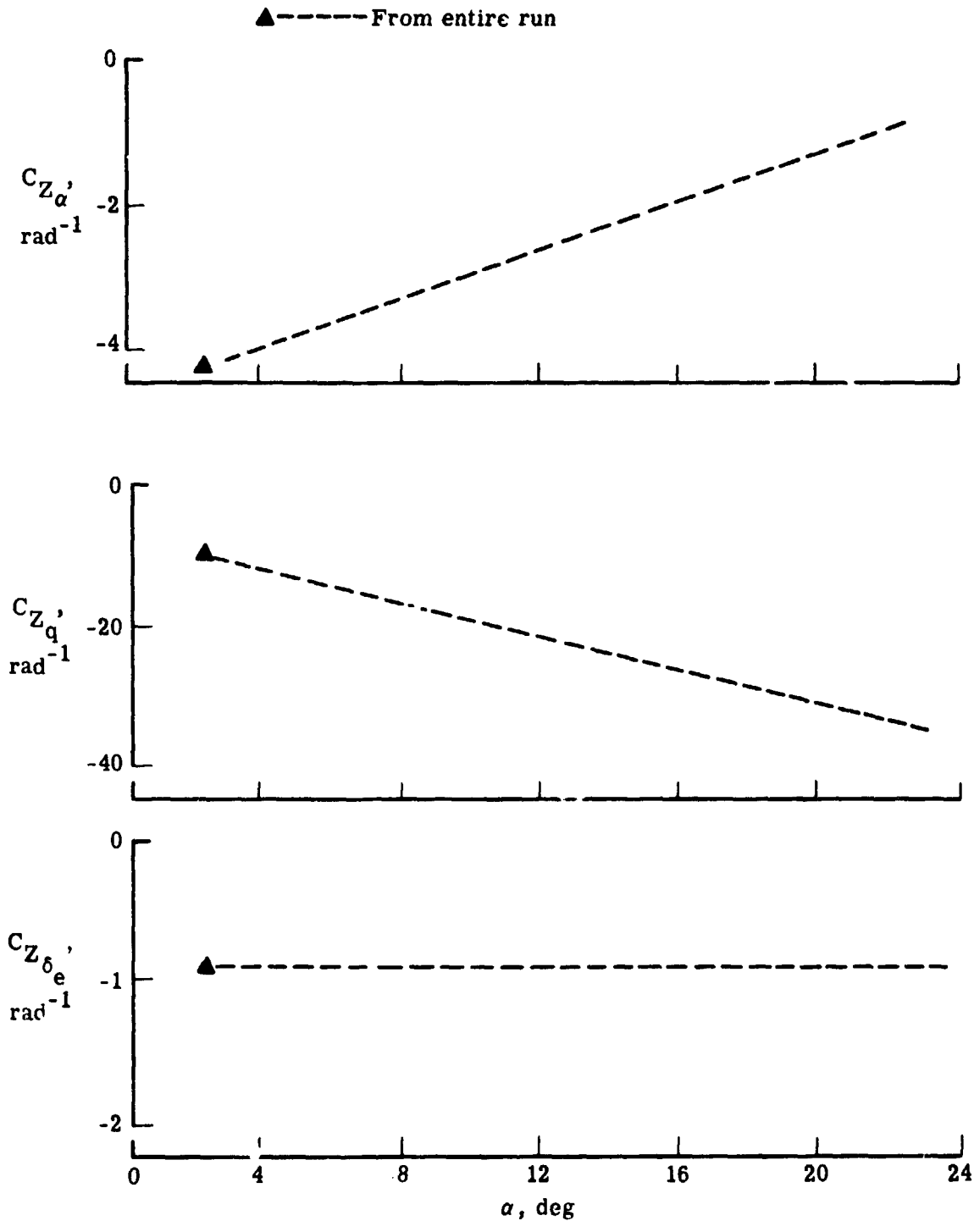

(a) Z-force coefficients.

Figure 3.- Aerodynamic coefficients from run 18 (large amplitude).

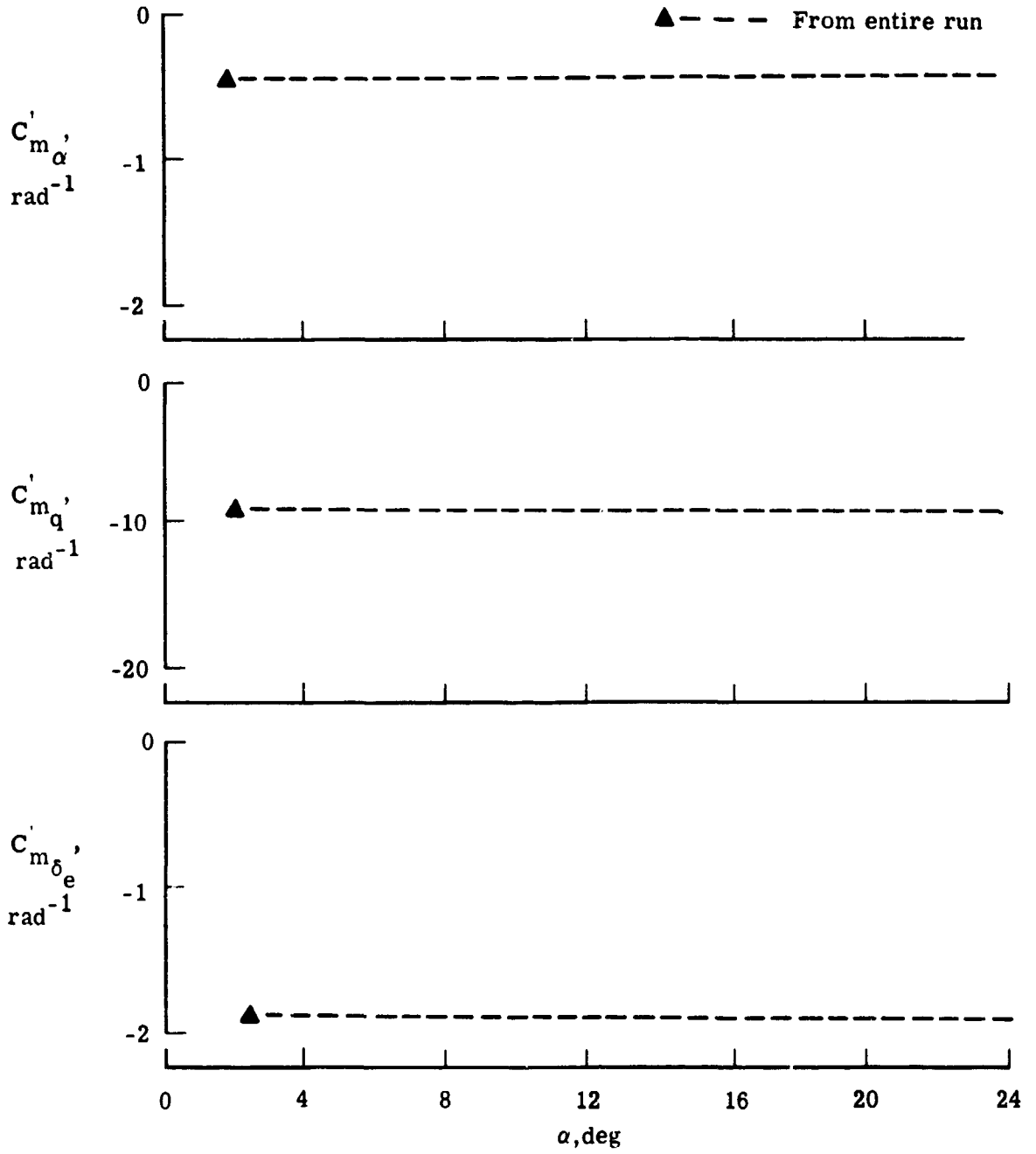

(b) Pitching-moment coefficient.

Figure 3.- Concluded.

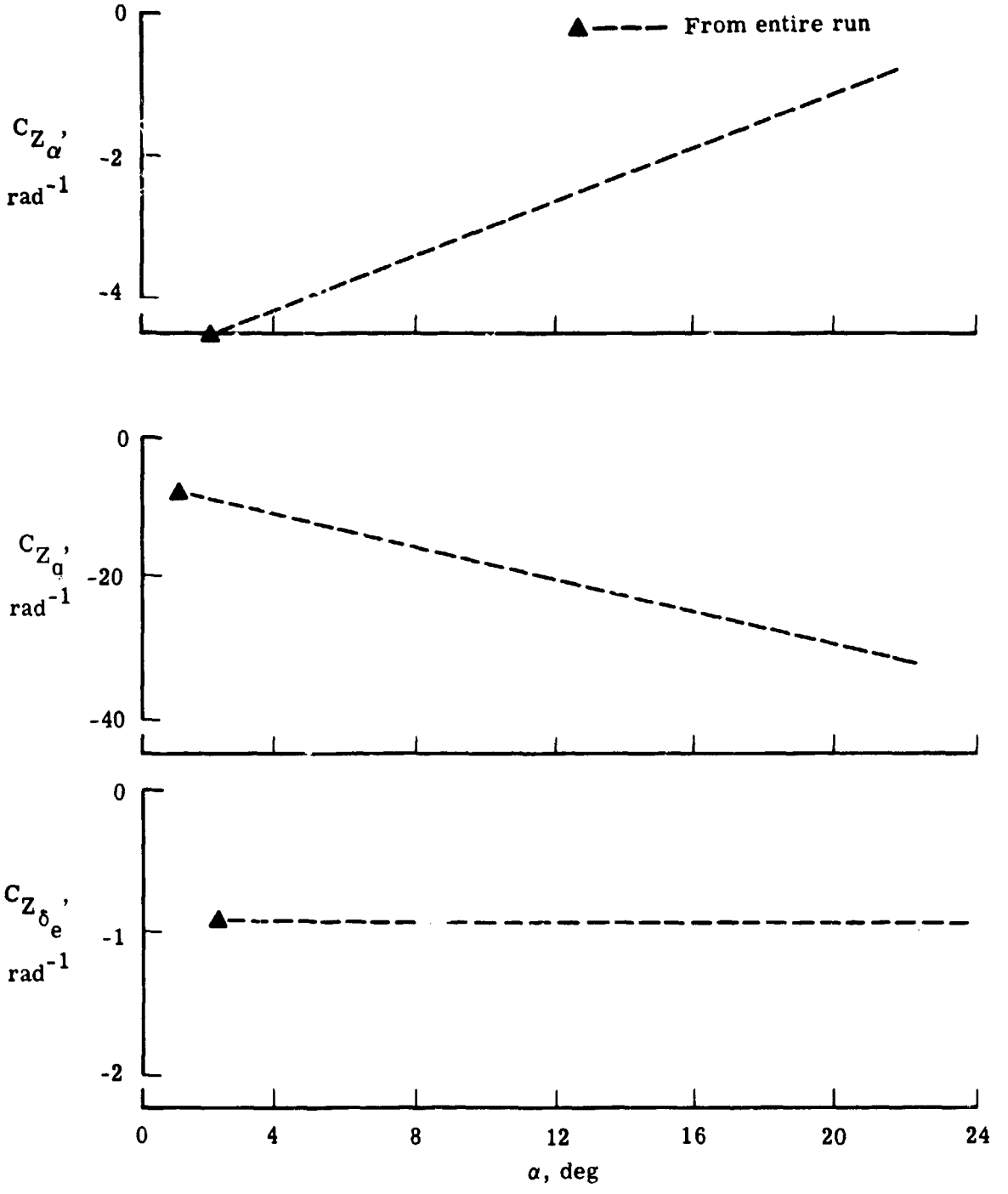

(a) Z-force coefficients.

Figure 4.- Aerodynamic coefficients from run 19 (large amplitude).

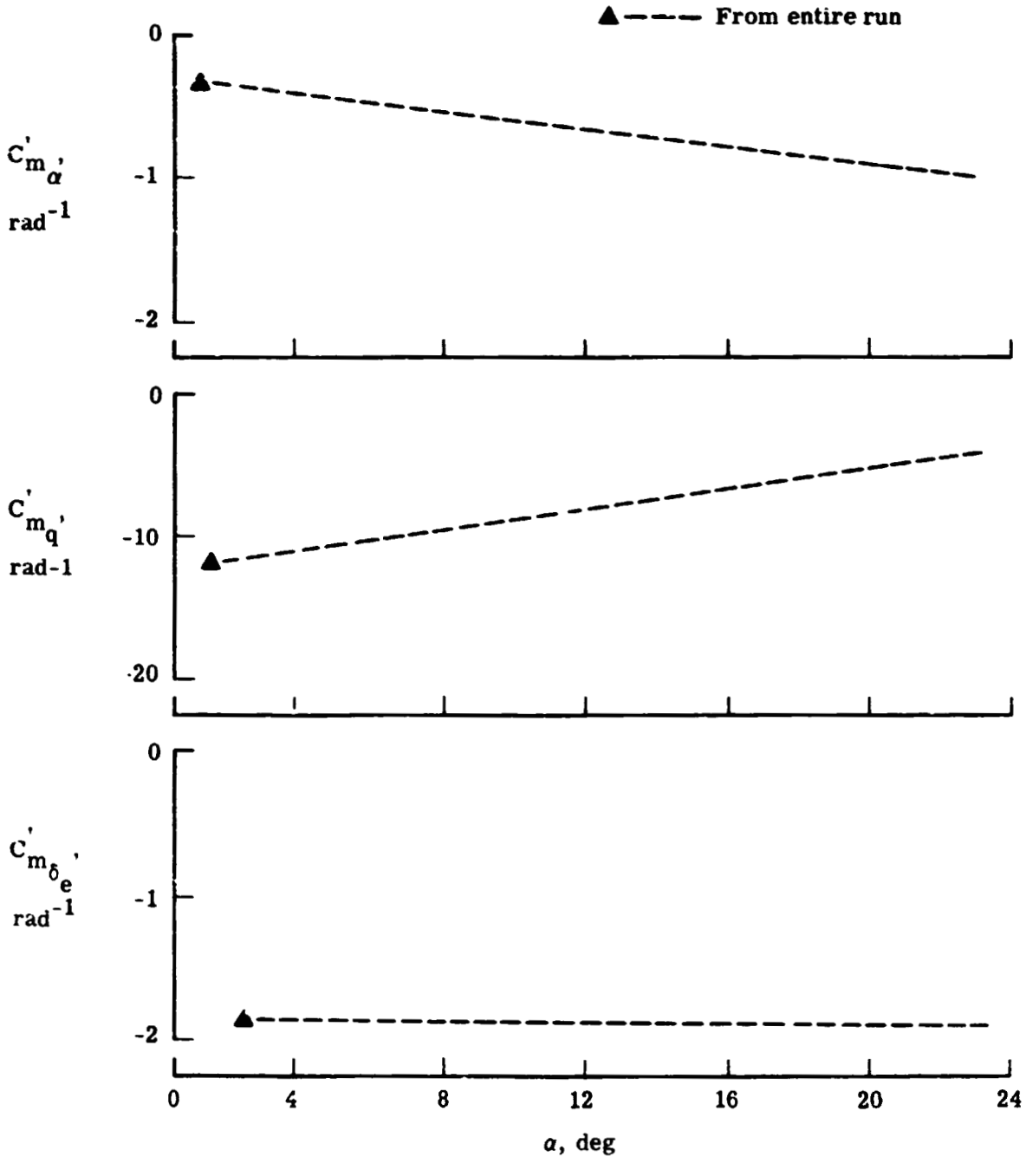

(b) Pitching-moment coefficients.

Figure 4.- Concluded.

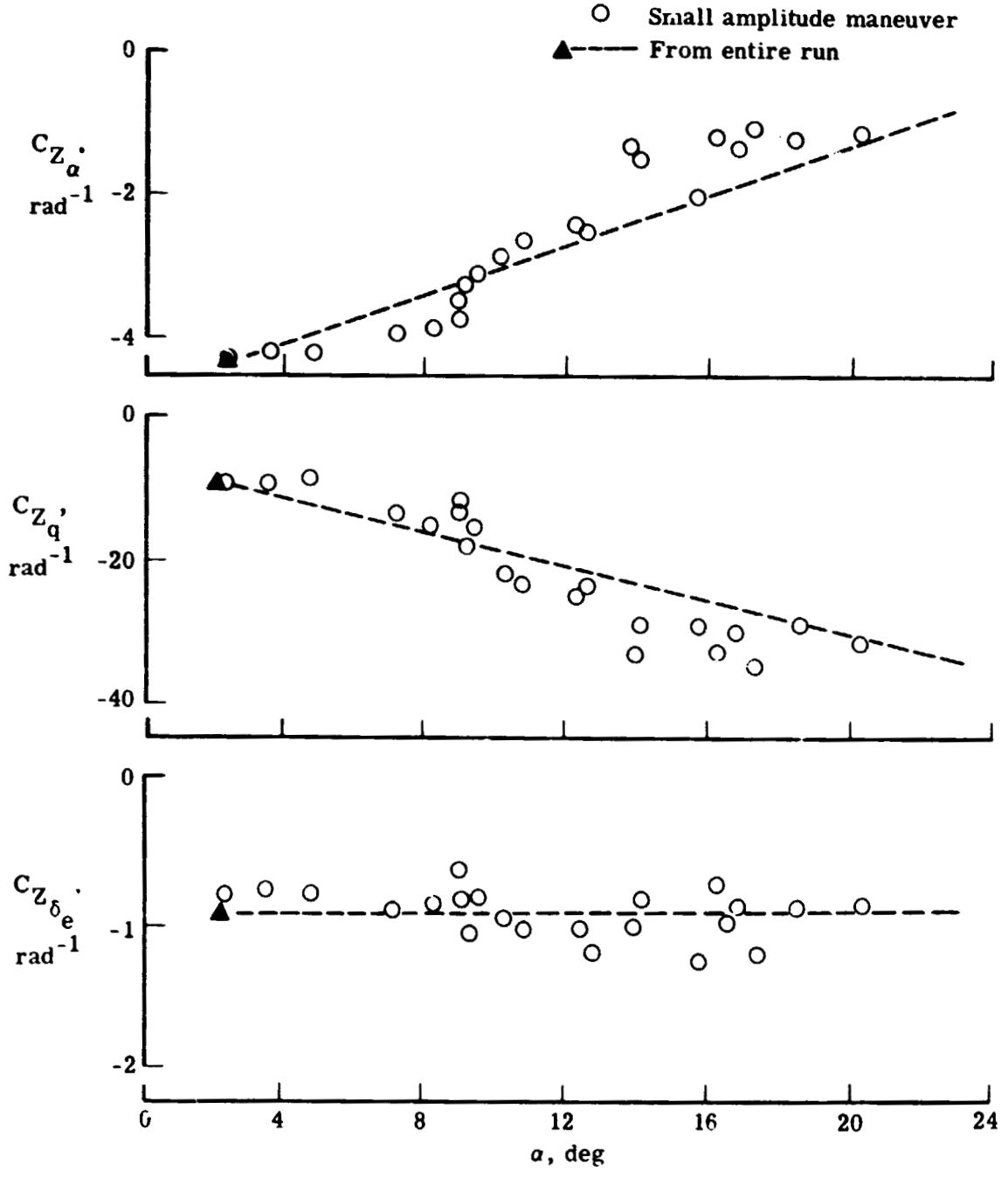

(a) Z-force coefficients.

Figure 5.- Comparsion of aerodynamic coefficients from run 18 and small amplitude maneuvers.

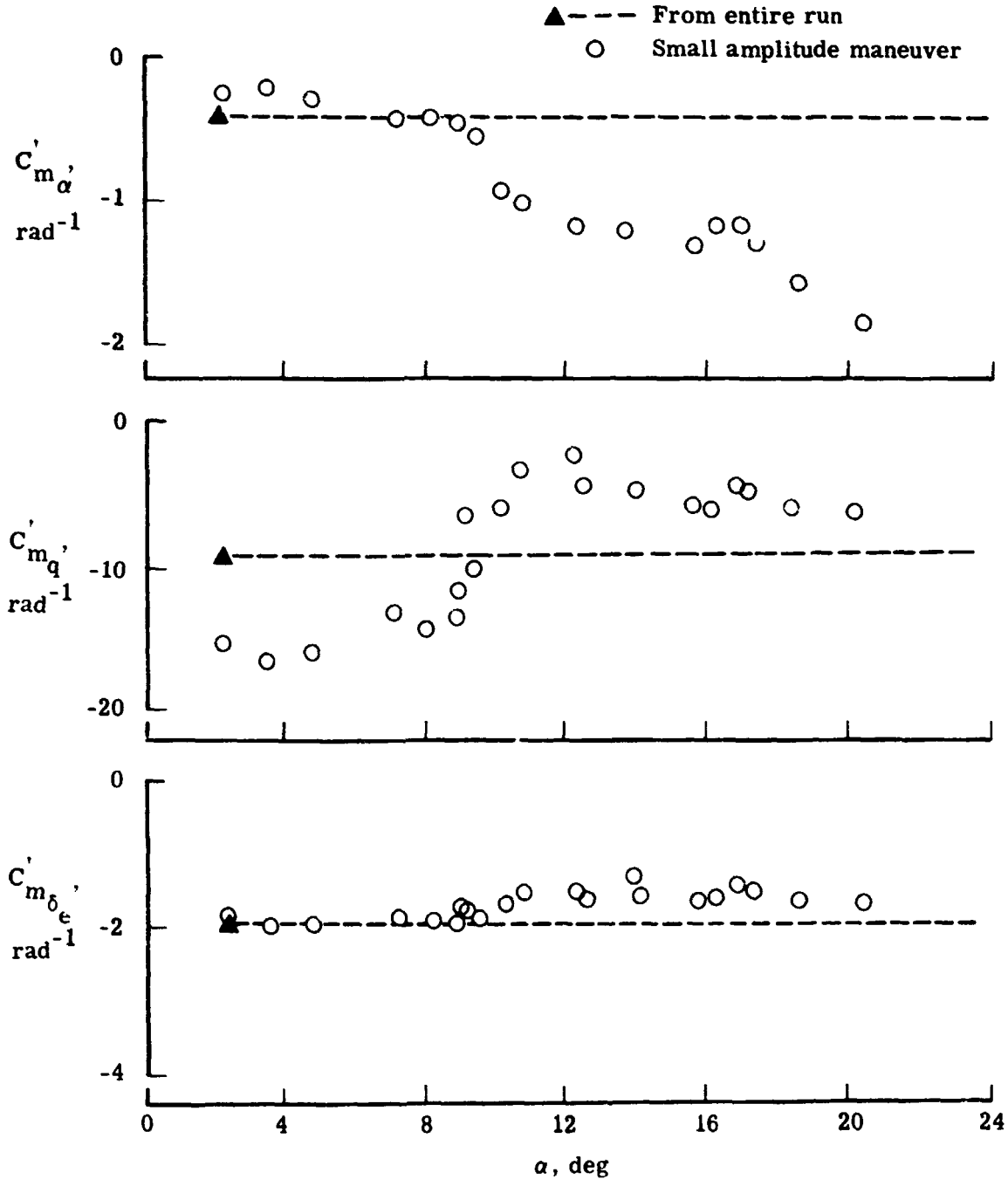

(b) Pitching-moment coefficients.

Figure 5.- Concluded.

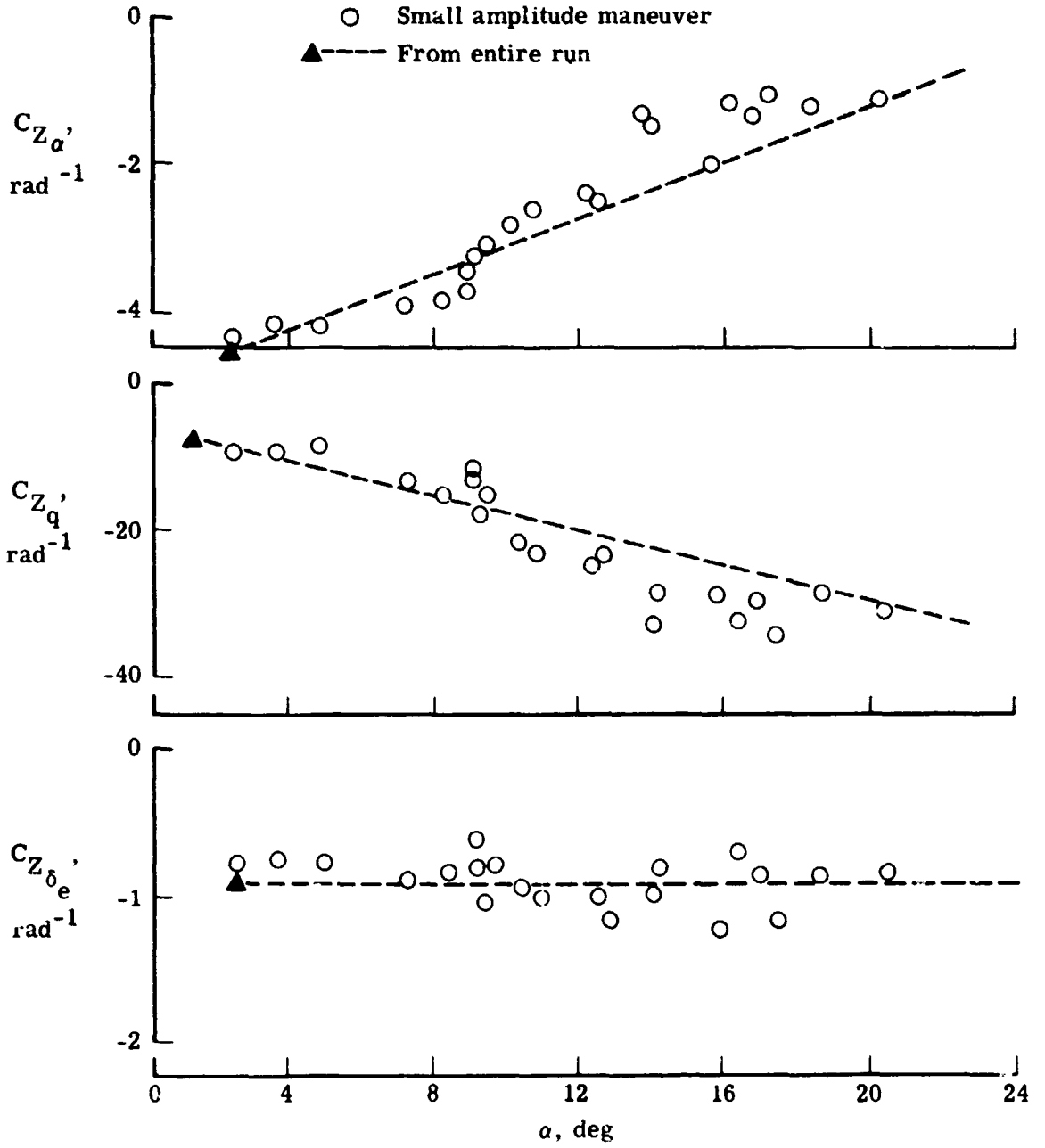

(a) Z-force coefficients.

Figure 6.- Comparison of aerodynamic coefficients from run 19 and small amplitude maneuvers.

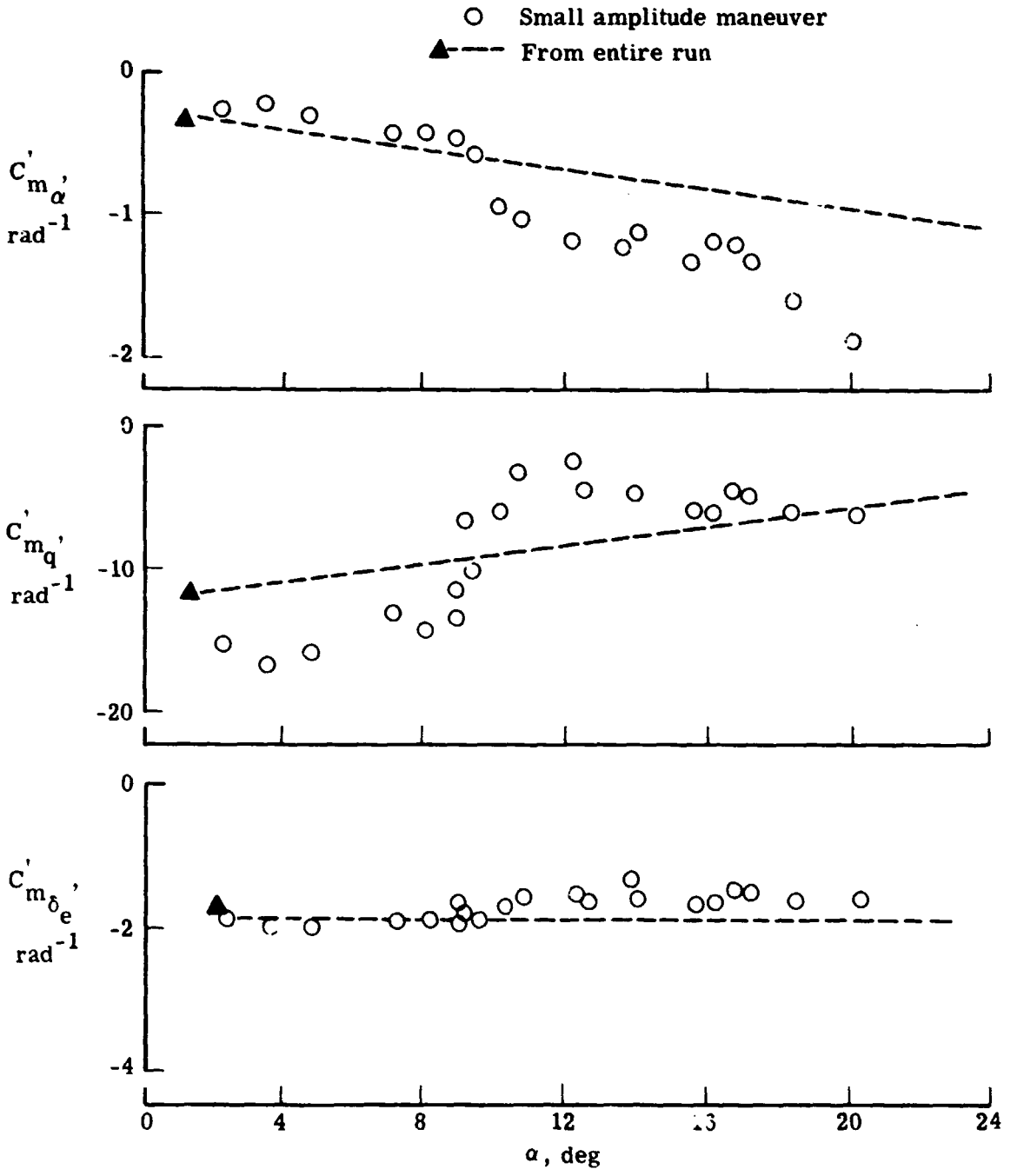

(b) Pitching-moment coefficients.

Figure 6.- Concluded.

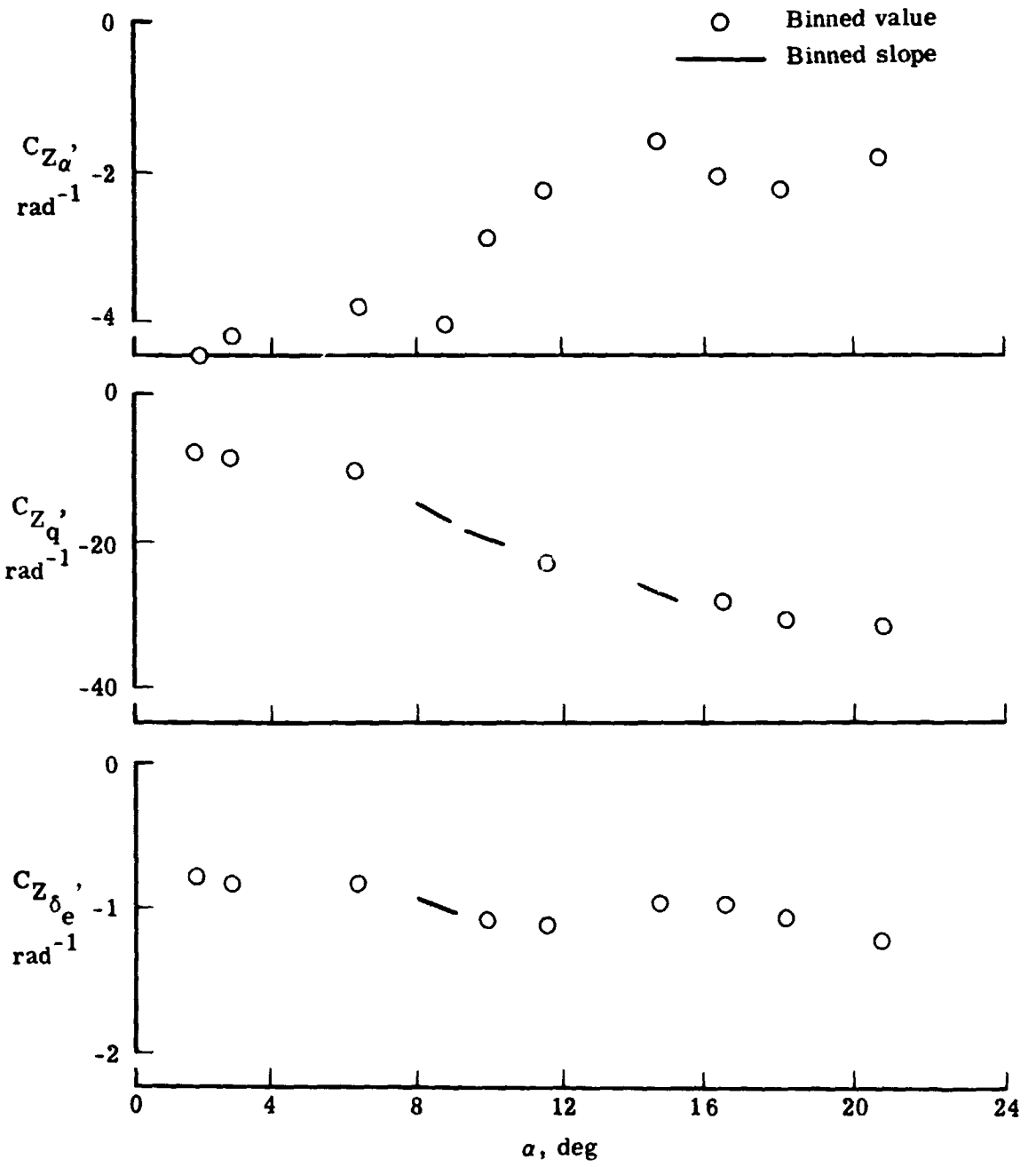

(a) Z-force coefficients.

Figure 7.- Aerodynamic coefficients from binned run 18.

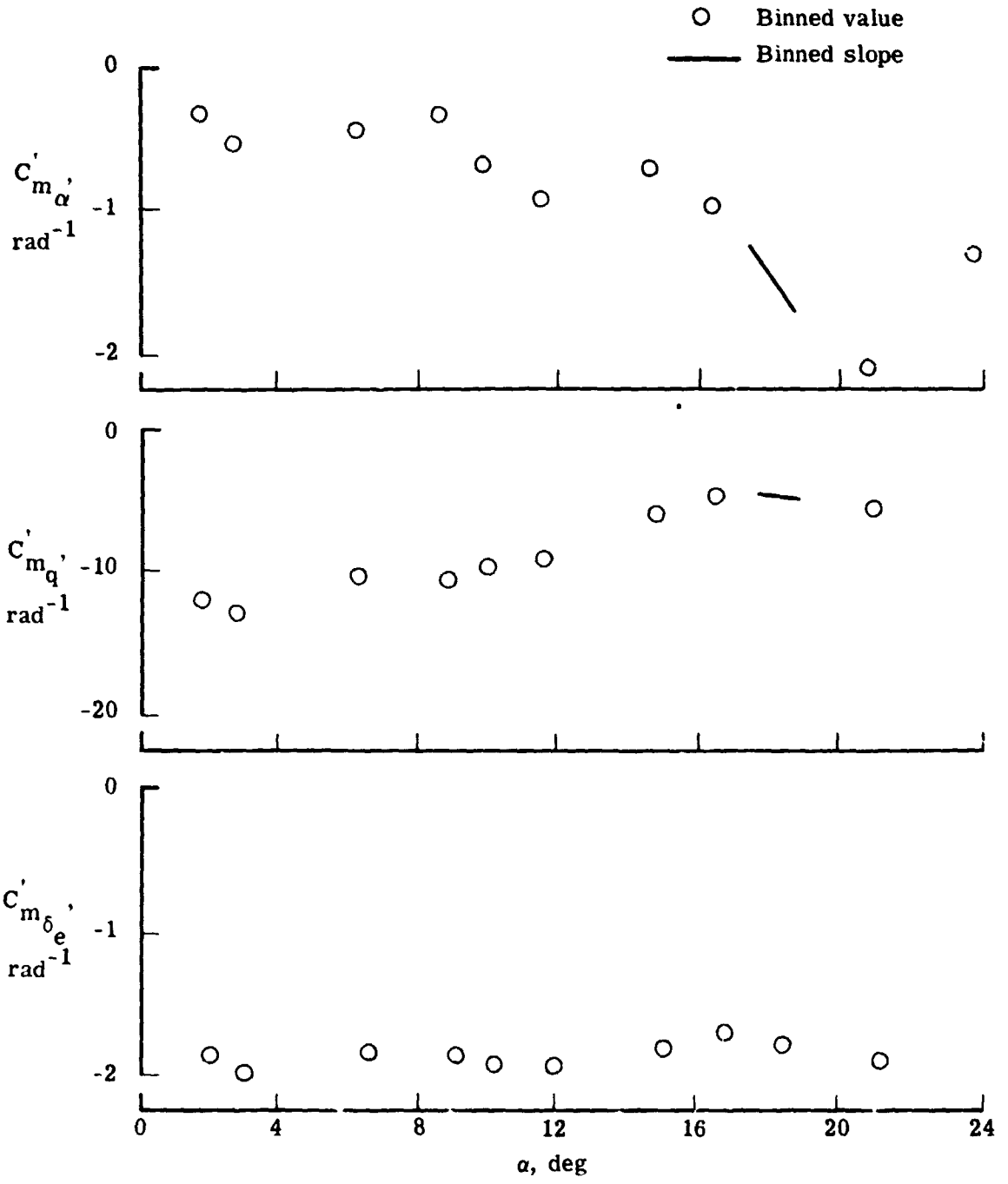

(b) Pitching-moment coefficients.

Figure 7.- Concluded.

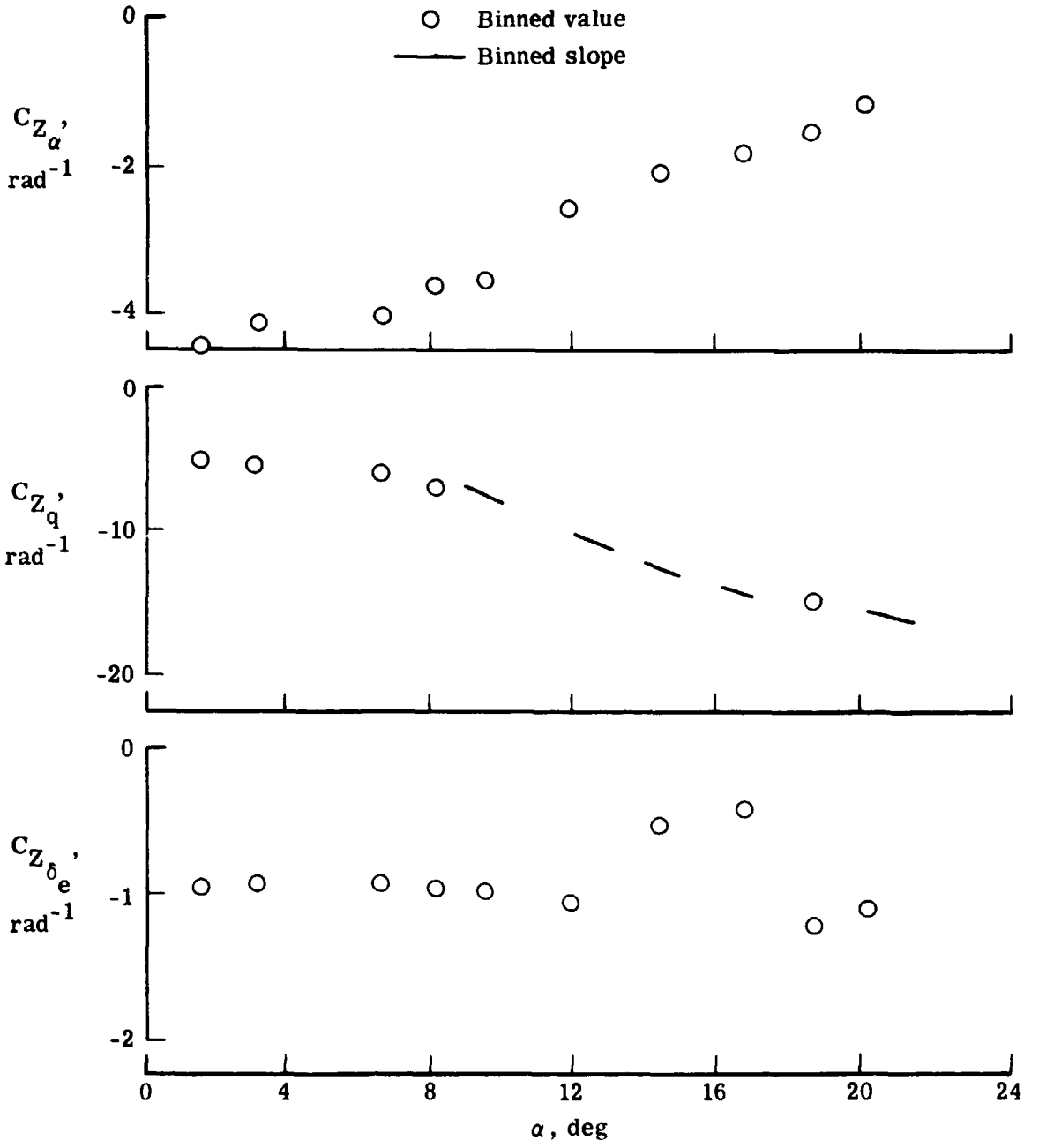

(a) Z-force coefficients.

Figure 8.- Aerodynamic coefficients from binned run 19.

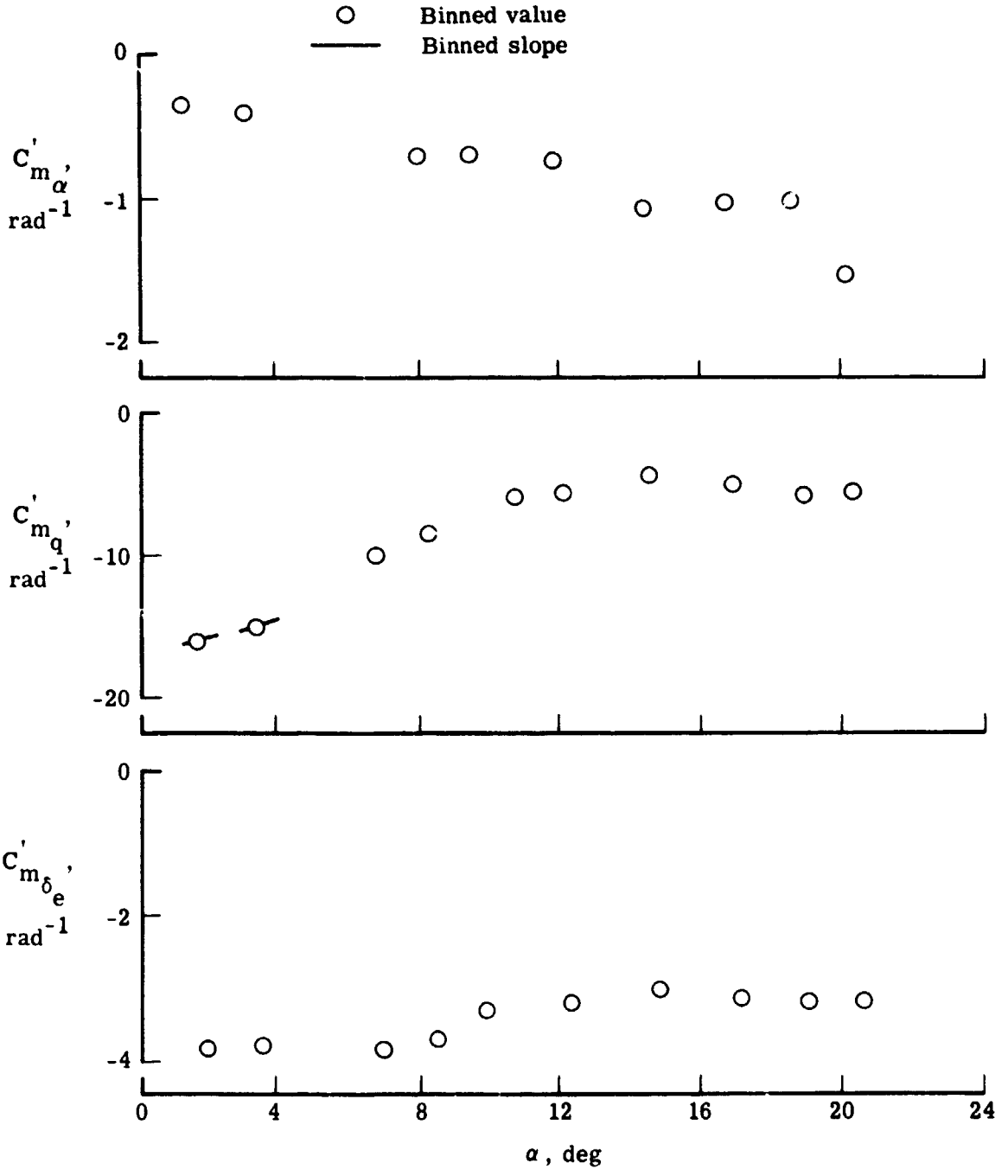

(b) Pitching-moment coefficients.

Figure 8.- Concluded.

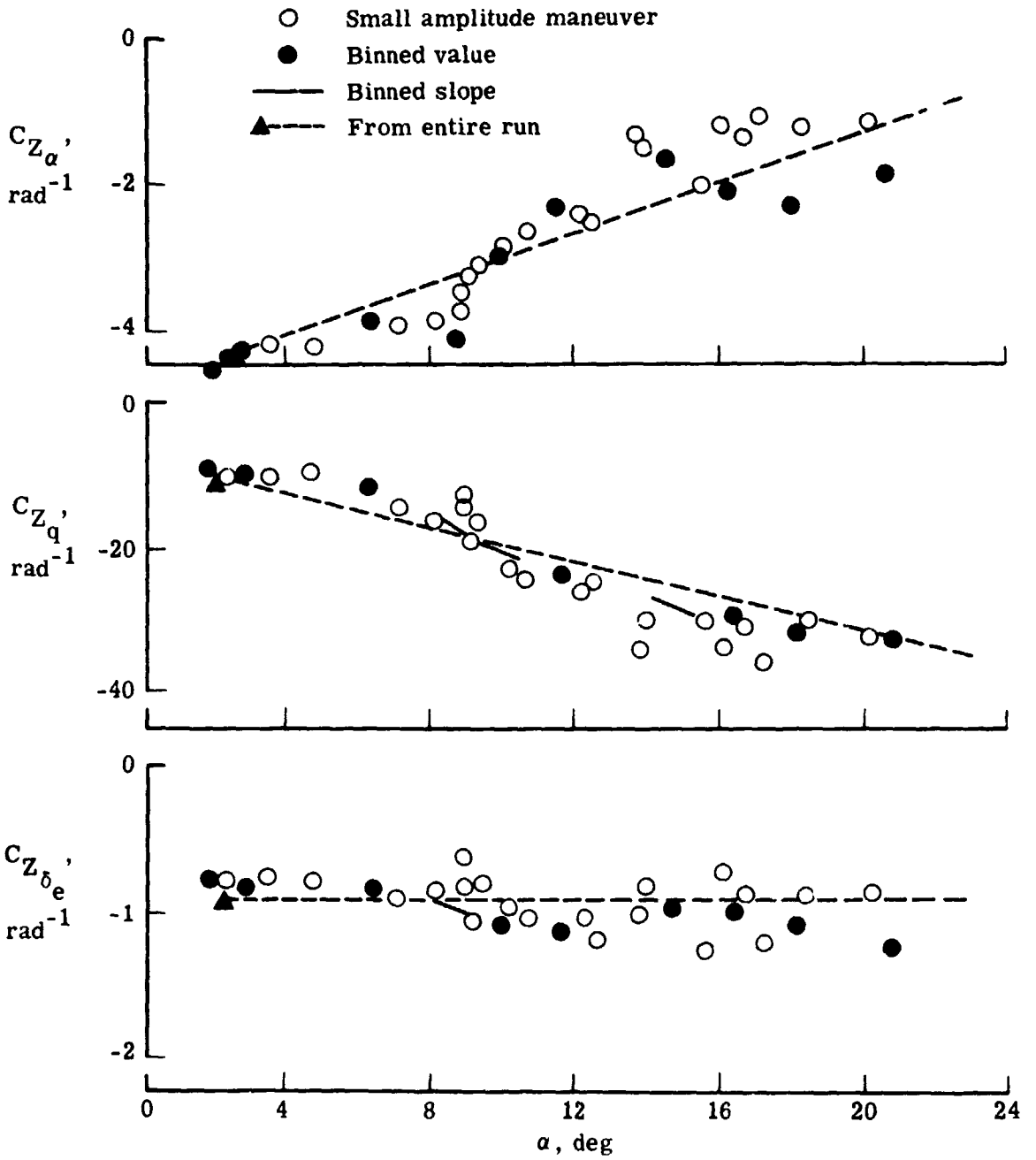

(a) Z-force coefficients.

Figure 9.- Comparison of aerodynamic coefficients from run 18 and small amplitude maneuvers.

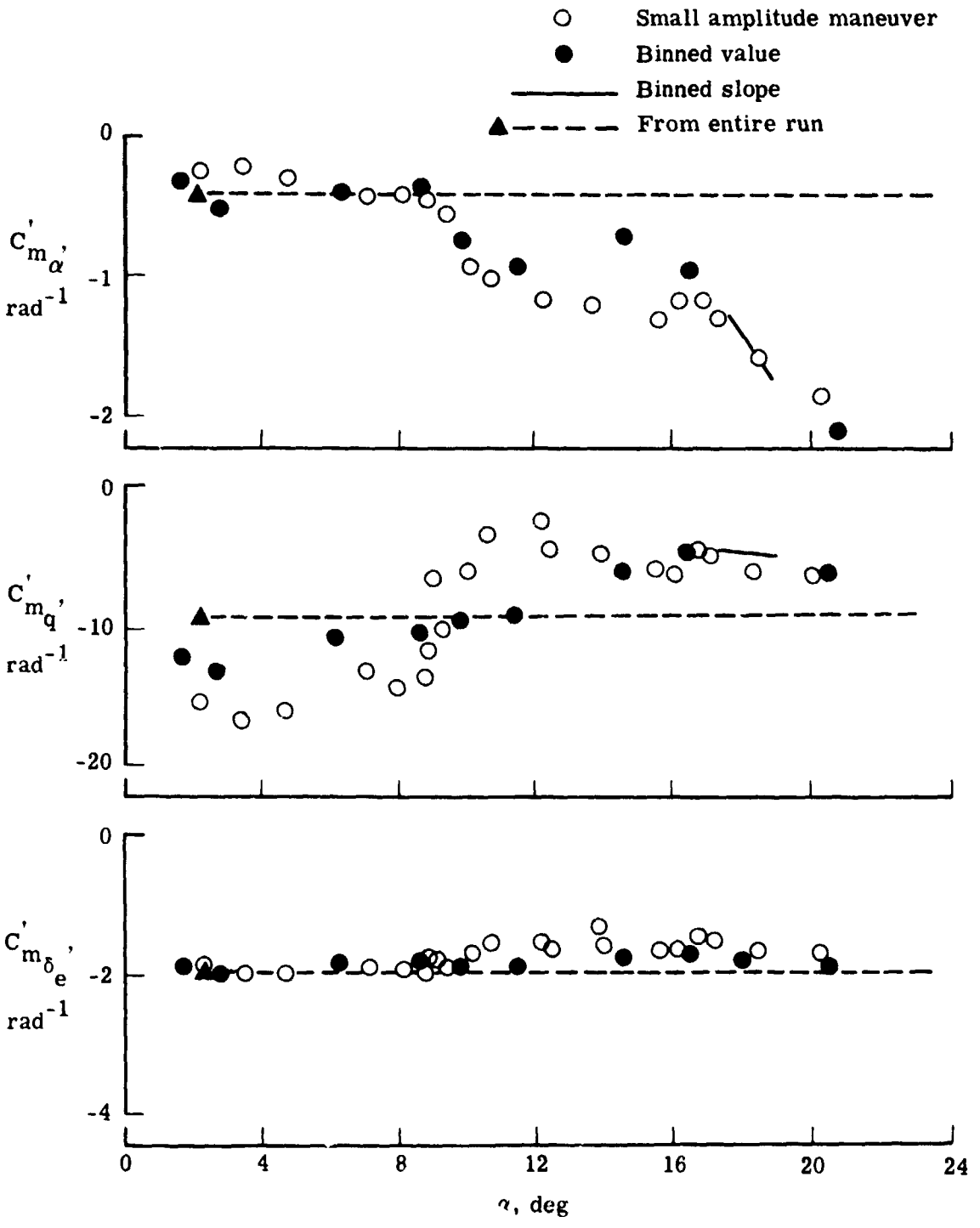

(b) Pitching-moment coefficients.

Figure 9.- Concluded.

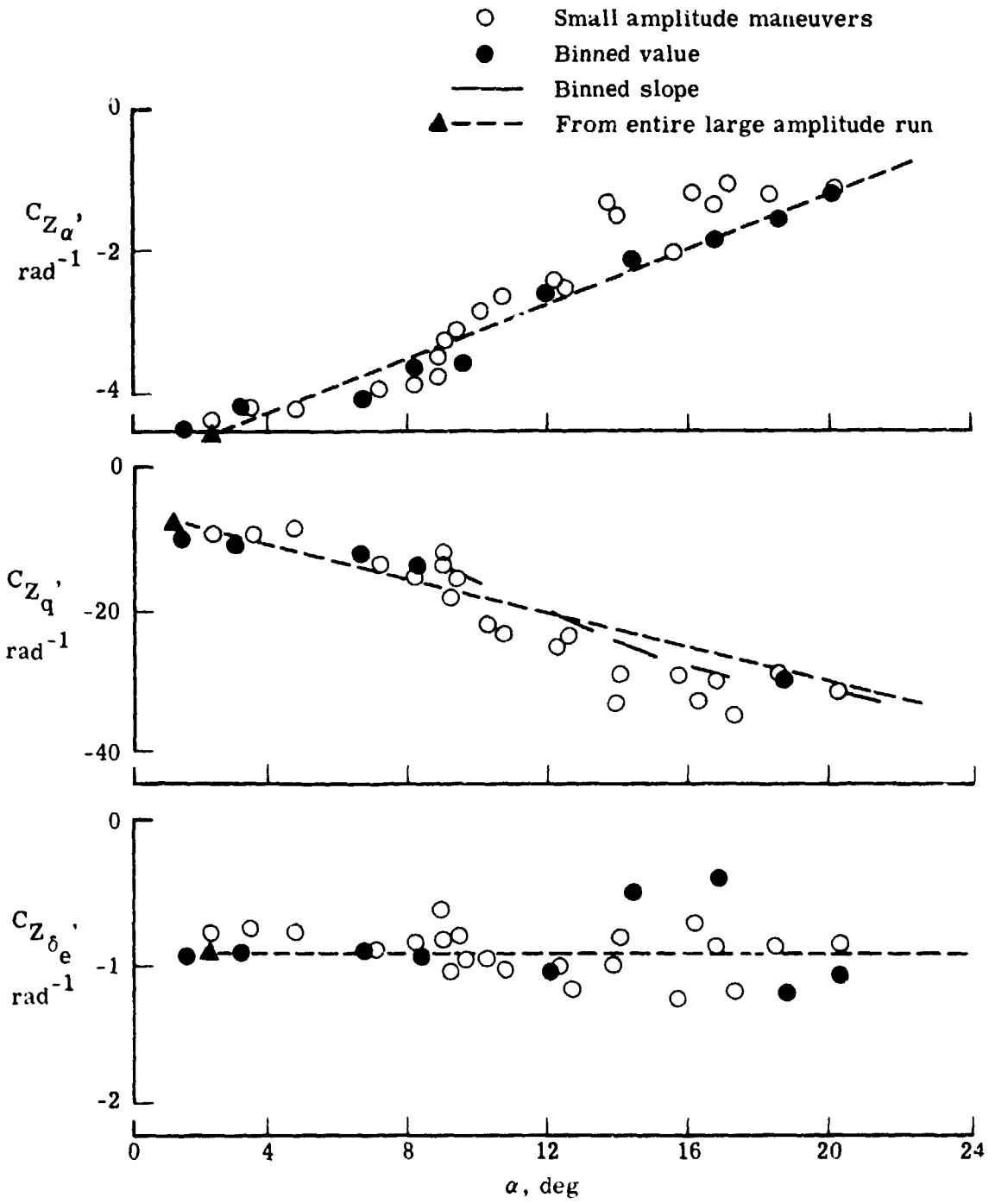

(a) Z-force coefficients.

Figure 10.- Comparison of aerodynamic coefficients from run 19 and small amplitude maneuvers.

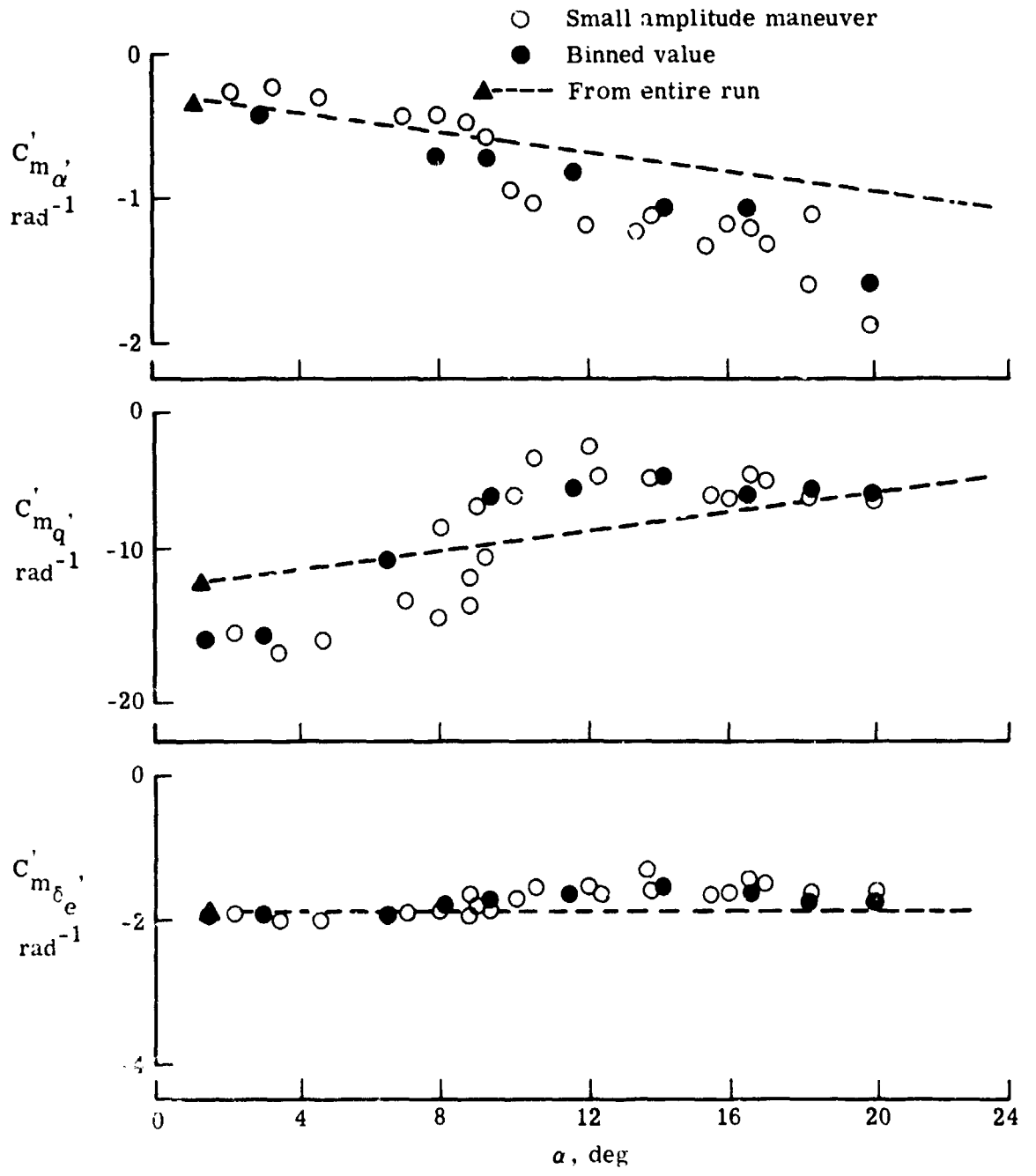

(b) Pitching-moment coefficients.

Figure 10.- Concluded.

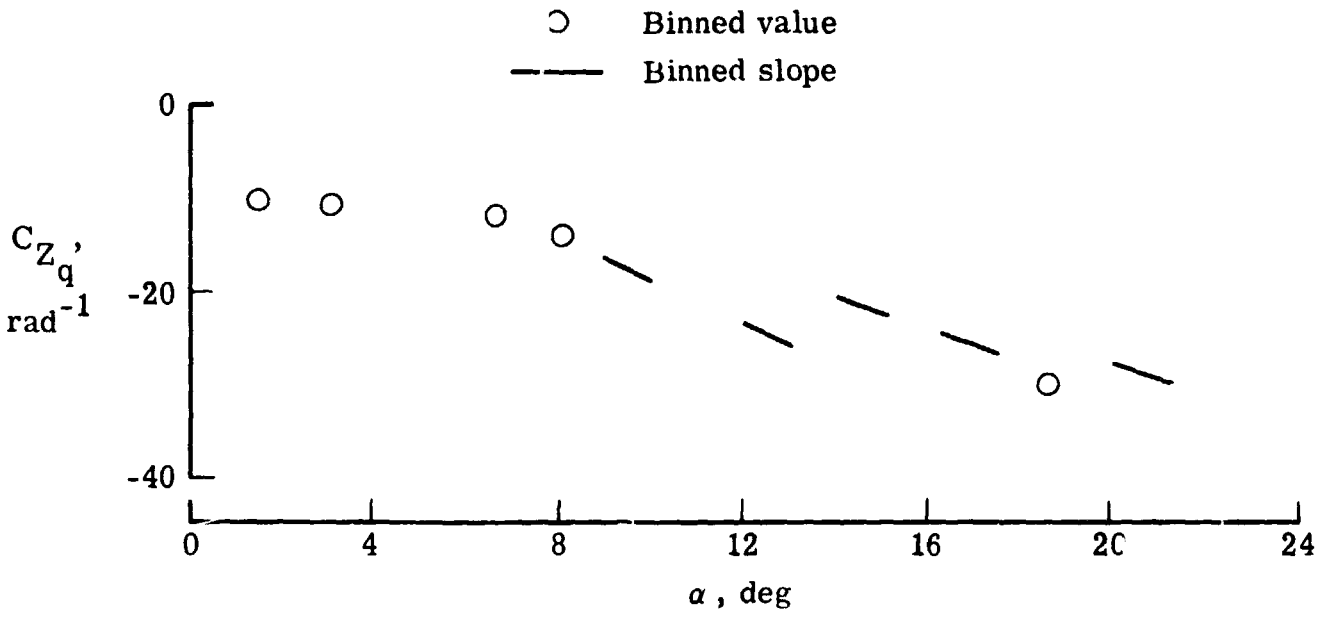

Figure 11.- Run 19 binned slope values for C_{Z_q} referenced to trim α.

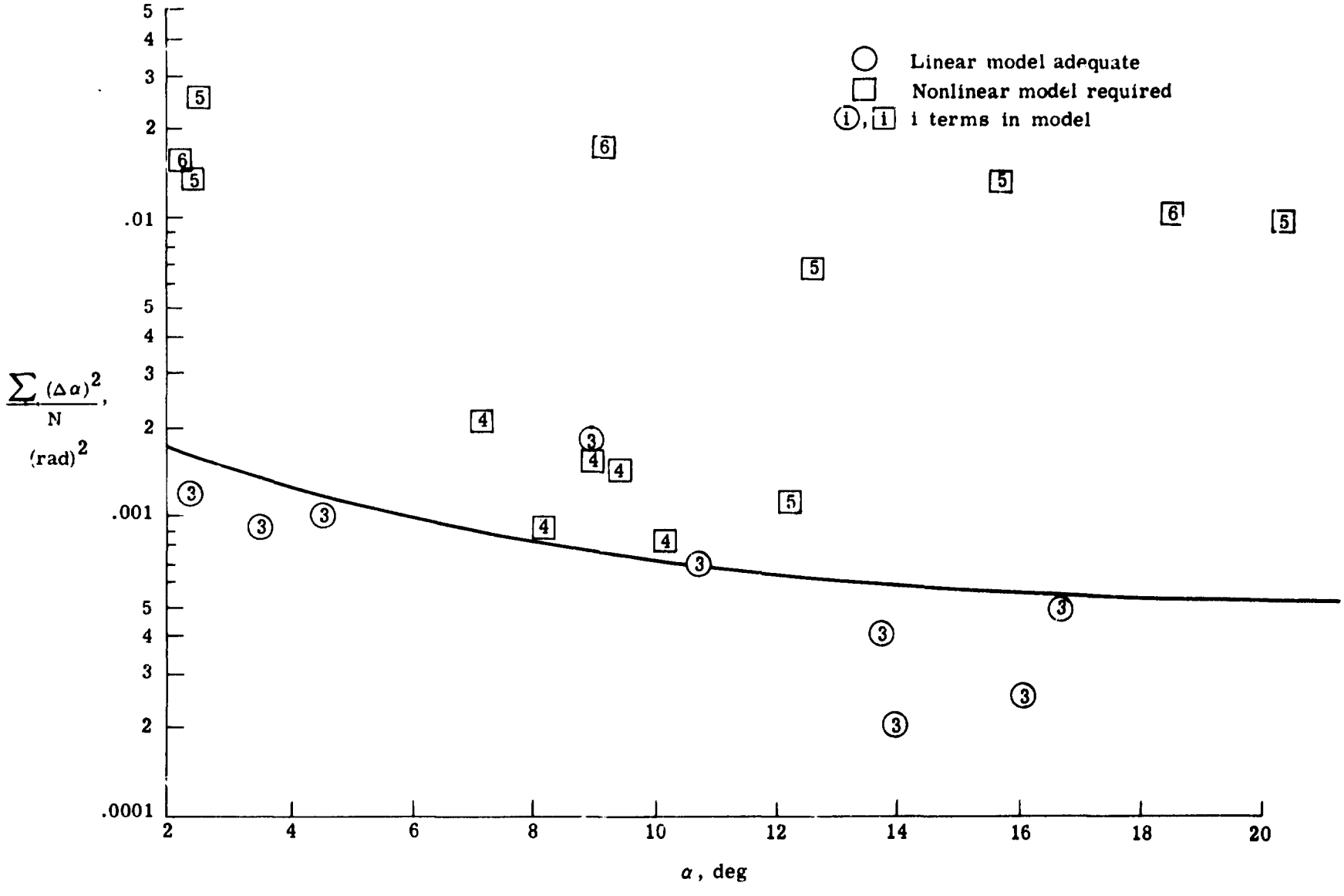

Figure 12.- Order of model as a function of trim α and average excursion in α for maneuver.